

# Inferior Parietal Lobule Projections to the Presubiculum and Neighboring Ventromedial Temporal Cortical Areas

SONG-LIN DING,<sup>1\*</sup> GARY VAN HOESEN,<sup>1,2</sup> AND KATHLEEN S. ROCKLAND<sup>1</sup>

<sup>1</sup>Department of Neurology, University of Iowa, Iowa City, Iowa 52242

<sup>2</sup>Department of Anatomy and Cell Biology, University of Iowa, Iowa City, Iowa 52242

---

---

## ABSTRACT

The entorhinal and perirhinal cortices have long been accorded a special role in the communications between neocortical areas and the hippocampal formation. Less attention has been paid to the presubiculum, which, however, is also a component of the parahippocampal gyrus, receives dense inputs from several cortical areas, and itself is a major source of connections to the entorhinal cortex (EC). In part of a closer investigation of corticohippocampal systems, the authors applied single-axon analysis to the connections from the inferior parietal lobule (IPL) to the presubiculum. One major result from this approach was the finding that many of these axons (at least 10 of 14) branch beyond the presubiculum. For 4 axons, branches were followed to area TF and to the border between the perirhinal and entorhinal cortices, raising the suggestion that these areas, which sometimes are viewed as serial stages, are tightly interconnected. In addition, the current data identify several features of presubicular organization that may be relevant to its functional role in visuospatial or memory processes: 1) Terminations from the IPL, as previously reported for prefrontal connections (Goldman-Rakic et al. [1984] *Neuroscience* 12:719–743), form two to four patches in the superficial layers. These align in stripes, but only for short distances ( $\approx 1.5$  mm). This pattern suggests a strong compartmentalization in layers I and II that is also indicated by cytochrome oxidase and other markers. 2) Connections tend to be bistratified, terminating in layers I–II and deeper in layer III. 3) Single axons terminate in layer I alone or in different combinations of layers. This may imply some heterogeneity of subtypes. 4) Individual axons, both ipsilateral projecting ( $n = 14$  axons) and contralateral projecting ( $n = 6$  axons), tend to have large arbors (0.3–0.8 mm across). Finally, the authors observe that projections from the IPL, except for its anteriormost portion, converge at the perirhinal-entorhinal border around the posterior tip of the rhinal sulcus. These projections partially overlap with projections from ventromedial areas TE and TF, and this convergence may contribute to the severe deficits in visual recognition memory resulting from ablations of rhinal cortex. *J. Comp. Neurol.* 425: 510–530, 2000. © 2000 Wiley-Liss, Inc.

**Indexing terms:** axon branching; entorhinal cortex; memory systems; perirhinal cortex; single axon reconstructions

---

---

The presubiculum is a multilayered, periallocortical structure located between the subiculum and the parasubiculum that is often considered part of the hippocampal formation. It receives connections from several cortical regions, including area 7a of the inferior parietal lobule (Seltzer and Van Hoesen, 1979; Seltzer and Pandya, 1984; Cavada and Goldman-Rakic, 1989), as well as areas in the prefrontal (Goldman-Rakic et al., 1984; Selemon and Goldman-Rakic, 1988; Morris et al., 1999) and cingulate cortices (Pandya et al., 1981) and the superior temporal gyrus (Amaral et al., 1983). Because a major efferent outflow from the presubiculum is to layer III of the ento-

rhinal cortex (EC), these cortical inputs are important as potential influences on the entorhinal-hippocampal component of the perforant pathway, including projections to

---

Grant sponsor: NINDS; Grant numbers: NS19632 and NS14944; Grant sponsor: NIMH; Grant number: MH53598.

\*Correspondence to: Song-Lin Ding, M.D., Department of Neurology, University of Iowa, 200 Hawkins Drive, Iowa City, IA 52242-1053. E-mail: slding@blue.weeg.uiowa.edu

Received 25 January 2000; Revised 12 June 2000; Accepted 14 June 2000

TABLE 1. Injection Parameters and Projection Foci<sup>1</sup>

Case	Weight (kg)	Sex	Injections	CA1		Presubiculum		Parasubiculum		Perirhinal and Endorhinal Cortices		
				Ipsi	Contra	Ipsi	Contra	Ipsi	Contra	Ipsi	Contra	
P5	4.0	M	2 (0.75, 1.2 μl), 18-day transport	+	NA	+++	NA	+	NA	++	+	NA
P6	6.0	F	1 (1.0 μl), 20-day transport	+	-	+++	++	(+)	-	++	+	+
P7	11.5	M	3 (1.0, 1.5, 1.7 μl), 25-day transport	++	+	++++	++	++	+	+++	++	NA (fibers in WM)
P8	4.6	F	2 (0.75, 1.25 μl), 26-day transport	++	-	+++	+	++	(+)	++	++	(+)
P9	5.7	F	1 (2.0 μl), 23-day transport	+	-	+++	-	++	-	++	+	-
P10	6.3	F	1 (1.2 μl), 29-day transport	(+)	NA	++	NA	-	NA	+++	++	NA
P11	6.6	F	4 (.5, .5, .75, .75 μl), 22-day transport	(+)	-	-	-	-	-	(+)	-	-

<sup>1</sup>Ipsi, ipsilateral; Contra, contralateral; M, male; F, female; +, relative density, where (+) is least and ++++ most dense; NA, not available.

the subiculum. They can be viewed as critical nontemporal corticohippocampal systems.

Recently, the presubiculum has attracted renewed interest because of the physiological demonstration in both rodents and monkeys (Taube et al., 1996; Robertson et al., 1999) that some neurons in this structure selectively increase their discharge rate when the subject's head is pointed, compass-like, in a best direction for that cell. The occurrence of "head-direction" cells bespeaks a role for the presubiculum in visuospatial processes. This would be compatible with the input to this region from the inferior parietal lobule (IPL), which has long been associated with visuospatial functions. It thus seemed important to further investigate the functional architecture of the presubiculum, with particular attention to the organization of the connections from the IPL.

The present study used single axon analysis to visualize and analyze the microarchitecture of parietal connections to the presubiculum. In particular, we were interested in establishing the size, configuration, and laminar termination of individual arbors and determining whether these might exhibit any features distinct from terminations in sensory cortical areas. Our results indicate that some parietal axons terminating in the presubiculum have relatively large arbors that often are distributed in distinct patches. Another finding was that many of these axons send branches to area TF and to the lateralmost border of the EC with the perirhinal cortex (PRh). This result was unexpected, because the presubiculum and area TF are generally viewed as serial stages in the corticohippocampal pathways. It implies that these "two" pathways can function as a tightly interconnected network.

**MATERIALS AND METHODS**

Tracer injections of biotinylated dextran amine (BDA) were placed in different portions of the inferior parietal lobule in two male (weight, 4 kg and 11.5 kg) and five female (weight, 4.6–6.6 kg) rhesus monkeys (*Macaca mulatta*). Animals were tranquilized with ketamine (11 mg/kg, i.m.) and were maintained under deep anesthesia with Nembutal (25 mg/kg, i.v.). Surgery was performed on anesthetized animals under sterile conditions and accord-

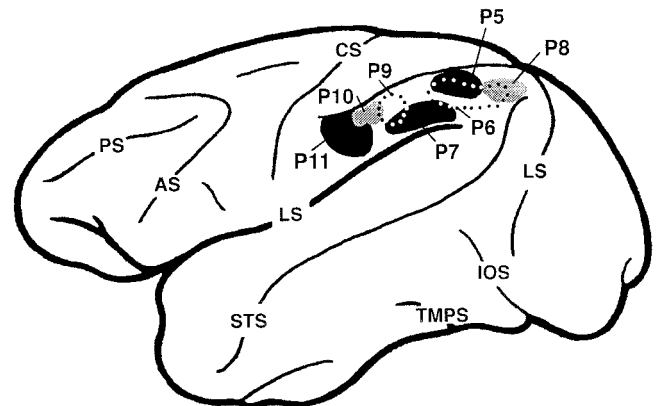


Fig. 1. Schematic view of the lateral surface of the monkey brain to show the distribution of seven injection sites (P5–P11) within the inferior parietal lobule (IPL). AS, arcuate sulcus; CS, central sulcus; LS, lateral sulcus; LS, lunate sulcus; IOS, inferior occipital sulcus; PS, principal sulcus; STS, superior temporal sulcus; TMPS, temporal middle posterior sulcus.

ing to institutional and U.S. Department of Agriculture guidelines, as specified in approved Animal Care and Use Forms (University of Iowa). Cortical areas of interest were localized by direct visualization, subsequent to craniotomy and durotomy, in relation to sulcal landmarks (i.e., the intraparietal and superior temporal sulci).

One to four pressure injections were made of BDA [10% in 0.0125 M phosphate-buffered saline (PBS), pH 7.2]. Equal parts of 10,000 and 3,000 molecular weight BDA (Molecular Probes, Eugene, OR) were used. Injections were deliberately made large to cover significant portions of a given cortical field and to optimize labeling of fine-caliber axons (see Table 1, Fig. 1). Multiple injections were placed close together so that they would merge into a single injection site. Animals were given postsurgical doses of antibiotic and analgesics, allowed to recover, and survived for 18–29 days. They were then reanesthetized with Nembutal (75 mg/kg) and perfused transcardially, in sequence, with 0.9% saline and 0.5% sodium nitrite; 4%

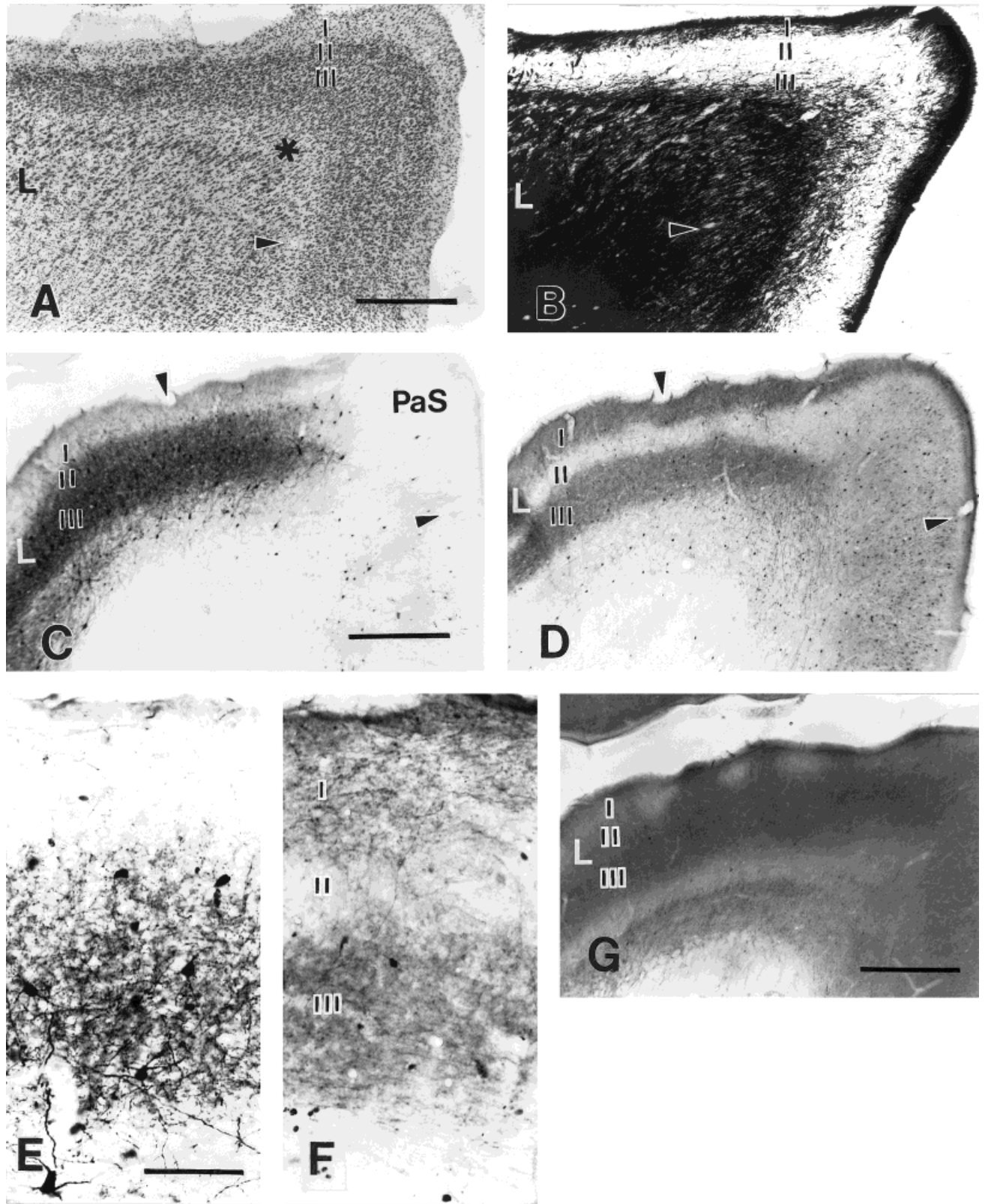


Fig. 2. Photomicrographs showing laminar organization of the presubiculum. **A:** Thionin stain for cell bodies. Asterisk indicates cell sparse lamina dissecans. **B:** Gallyas stain for myelin. A and B are from closely adjacent sections, and arrowheads point to corresponding blood vessels. **C:** Immunocytochemistry (icc) for parvalbumin (Parv). **D:** Icc for calbindin (CB). C and D are from adjacent sections, and arrowheads point to corresponding features. **E,F:** Higher magnifica-

tion photomicrographs of closely adjacent sections reacted for Parv (E) and for CB (F). **G:** Section reacted for cytochrome oxidase. Patches are evident in layer I and in the superficial part of layer II. PaS, parasubiculum; L, lateral (edge of the presubiculum). Scale bars = 500  $\mu$ m in A (also applies to B), C (also applies to D), G; 100  $\mu$ m in E (also applies to F).

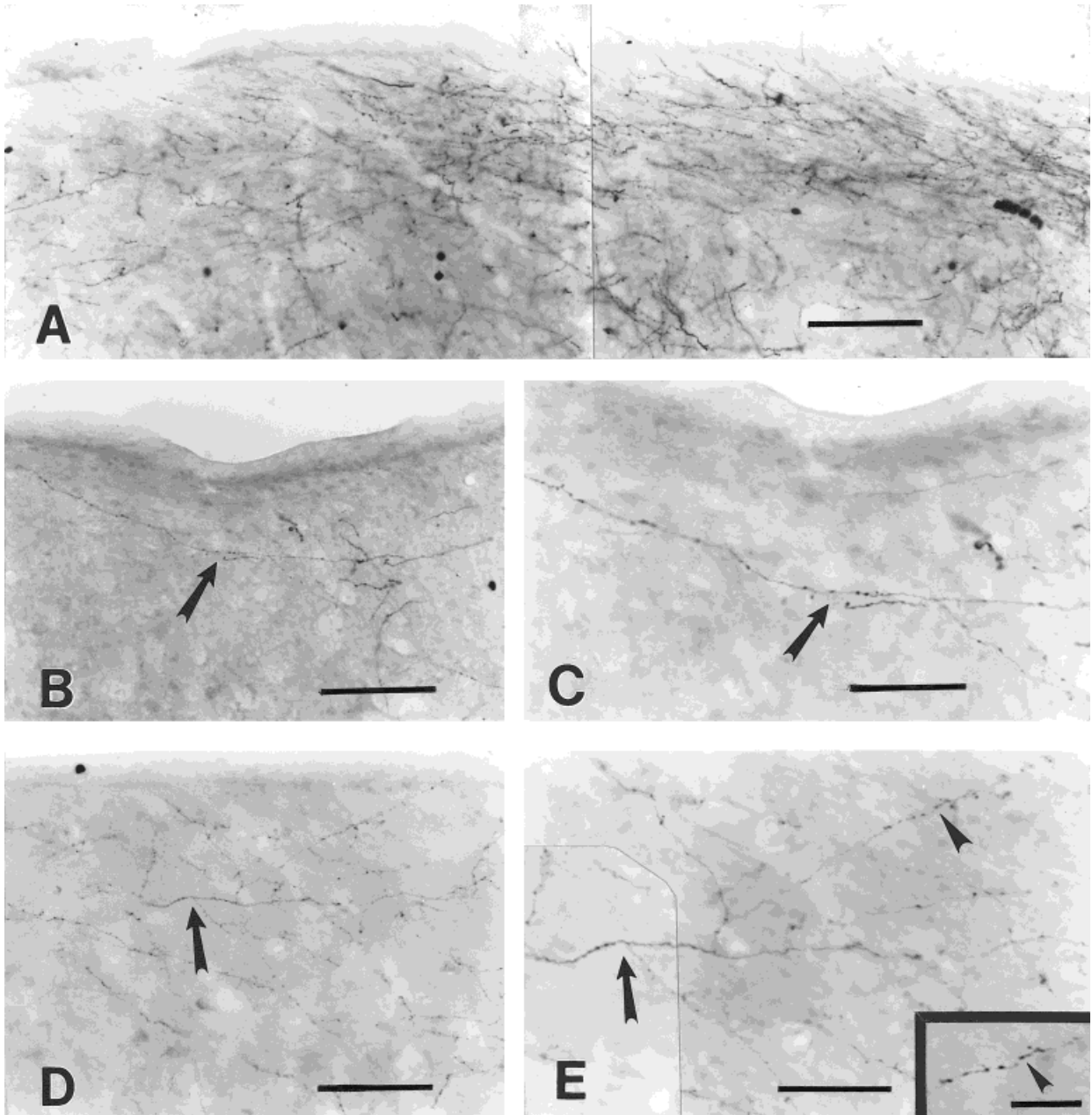


Fig. 3. **A:** Photomicrograph of terminations in layer I of the presubiculum from case 7. **B:** Portion of a labeled axon in layer I from case 5. **C:** Higher magnification view of the area indicated by the arrow in B. **D:** Portion of another labeled axon in layer I (two focal planes have been montaged together). **E:** Higher magnification view of

the area indicated by the arrow in D. The camera lucida reconstruction of this axon is illustrated in Figure 9A. **Inset** in E is higher magnification view of terminal specializations (arrowhead points to corresponding features in E and inset). Scale bars = 100  $\mu$ m in A,B,D; 50  $\mu$ m in C,E; 20  $\mu$ m in inset.

paraformaldehyde; and chilled 0.1 M phosphate buffer with 10%, 20%, and 30% sucrose. For two of the animals (P5 and P7), 0.25% glutaraldehyde was added to the fixative.

Brains were cut serially in the coronal plane by frozen microtomy (at 50  $\mu$ m thickness) and processed histologically for BDA (Brandt and Apkarian, 1992; Veenman et al., 1992). Tissue was reacted for 20–24 hours in avidin-biotin complex (ABC) solution (Vector Laboratories, Bur-

lingame, CA) at room temperature (ABC Elite kits; 1 drop of reagents per 7 ml of 0.1 M PBS). In the final step, BDA was demonstrated by 3,3'-diaminobenzidine tetrahydrochloride (DAB) histochemistry with the addition of 0.5% nickel-ammonium sulfate.

### Analysis

This study emphasizes serial section reconstruction of single axons terminating in the presubiculum. Recon-

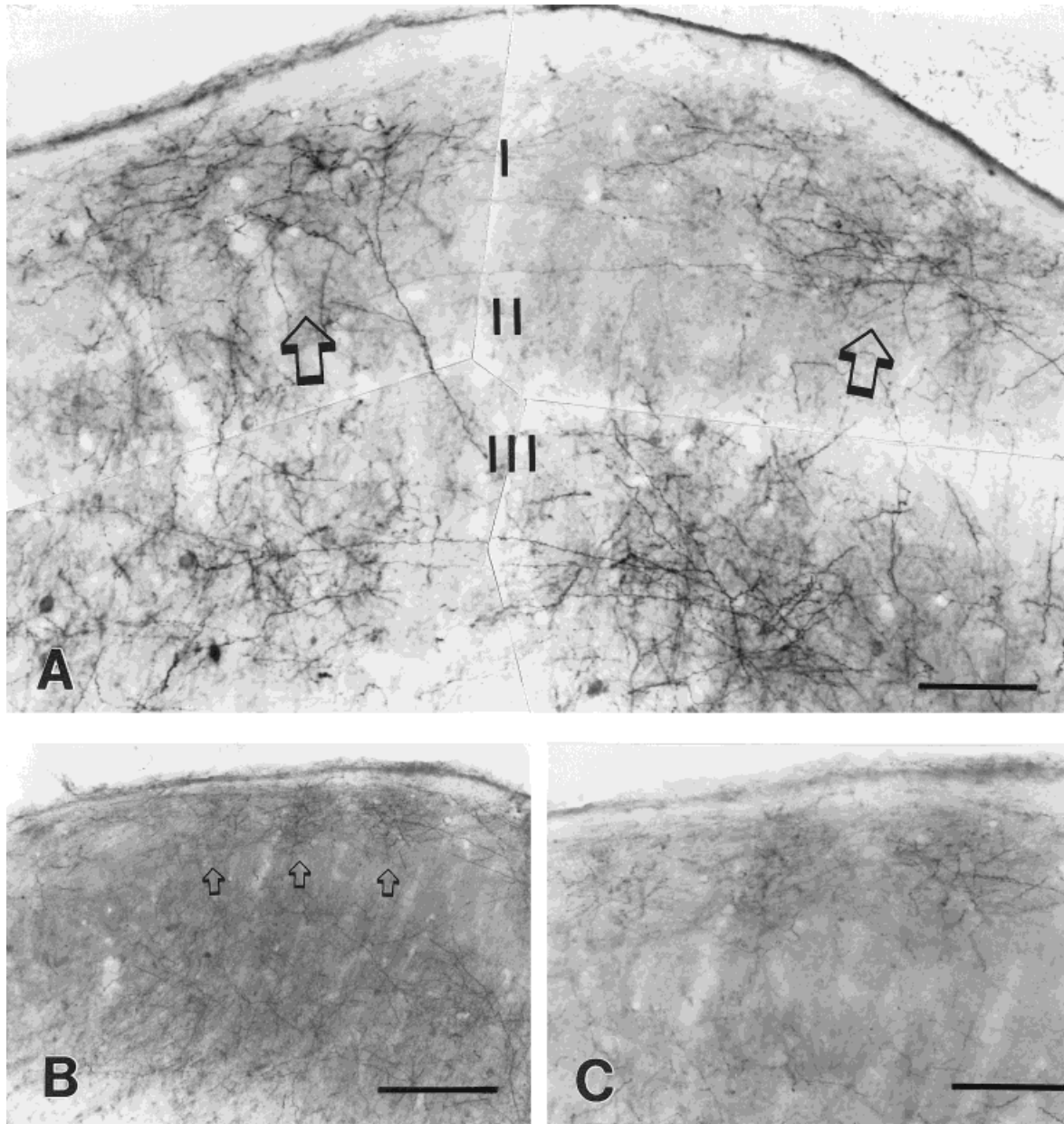


Fig. 4. Photomicrographs showing bistratified distribution of terminal labeling. **A:** Terminations are concentrated in layers I and upper III (from case 9). A few neurons retrogradely filled from the biotinylated dextran amine (BDA) injection are evident in layer III at

the left. **B:** Three distinct terminal patches are evident in layers I and II (from case 9). **C:** Higher magnification view of the section shown in B. Arrows in A and B point to terminal patches. Scale bars = 100  $\mu\text{m}$  in A,C; 200  $\mu\text{m}$  in B.

structions were carried out with the aid of a camera lucida microscope attachment (BH-2 microscope; Olympus, Tokyo, Japan). Axons were drawn on paper at magnifications of  $\times 100$  and  $\times 600$  (oil-immersion). Complex portions of the axon (i.e., branch points or crowded fields) were drawn and/or verified under oil immersion at  $\times 1,000$  magnification. The overall projection focus in each case was also charted for extent, pattern, and laminar organization.

The presubiculum and entorhinal cortex were readily identified by their specialized lamination. This was visualized by light cellular background staining from DAB

and/or Nomarsky optics. Nissl counterstains were only occasionally used, as they tended to camouflage fine axonal processes and preclude any further reconstructions. Other fields, including the localization of injection sites within the IPL, were identified by architectonic features (in counterstained material), by overall connectivity patterns, and by comparison with published mapping studies. The series of injections in the IPL was designed to cover this region in both the mediolateral (ML) and anteroposterior (AP) axes (except for the most posterior sector, which has been considered as a component of the occipital

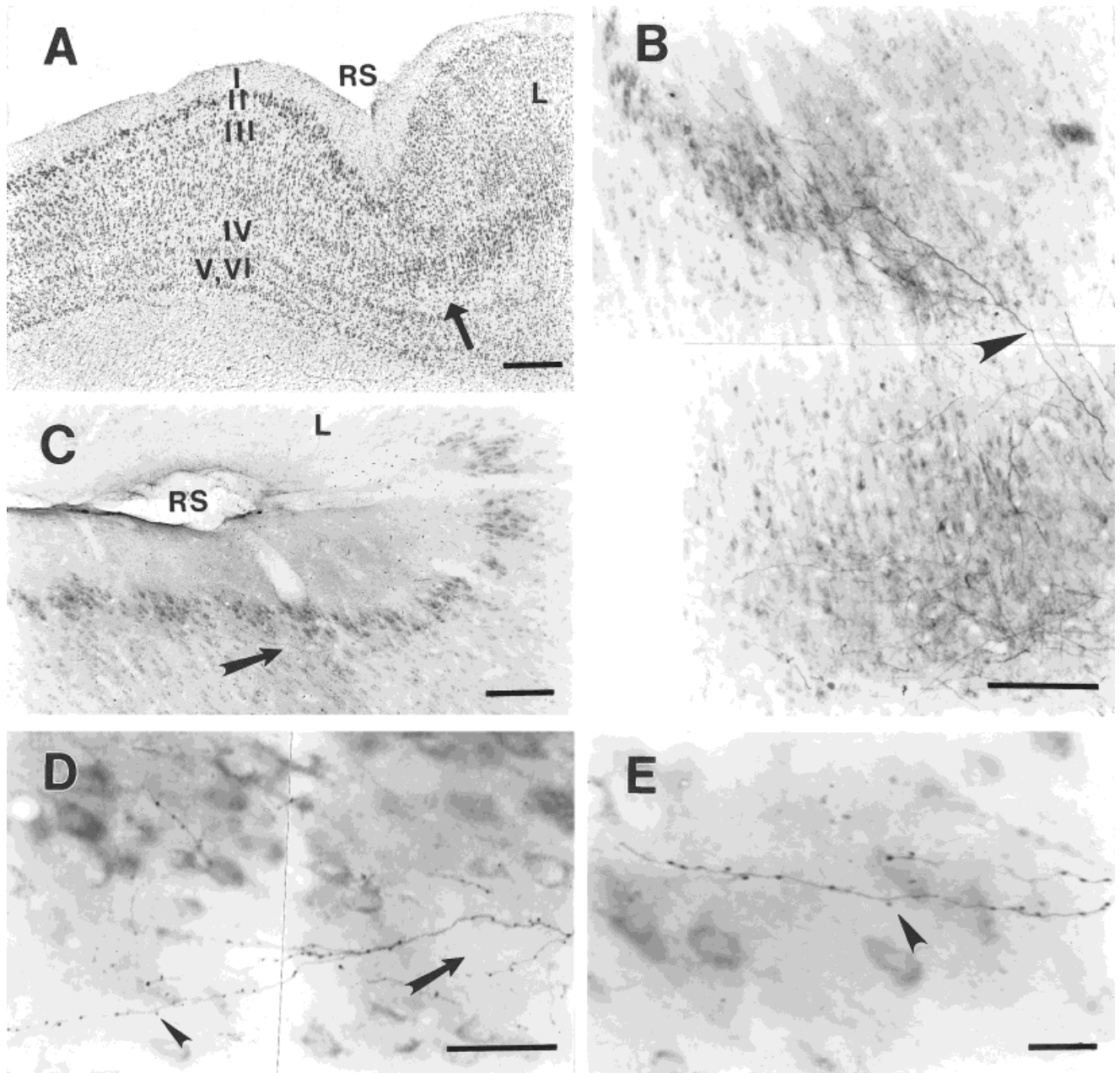


Fig. 5. Photomicrographs of the border between the perirhinal (PRh) and entorhinal (ERh) cortices (arrow in A) at the posterior tip of the rhinal sulcus (RS). **A:** Thionin stain for cell bodies. **B:** Terminal labeling (from case 9) in the depth of the rhinal sulcus (RS) at the border between the PRh (right) and ERh (left) cortices. Arrowhead points to an isolated branch from a single axon. **C:** Single axon (from case 9) terminating in layer II/III of the medial bank of the RS.

(The lateral surface is at the top and is rotated 90° from A and B). **D:** Higher magnification of C (arrows point to corresponding features). **E:** Higher magnification of D (arrowheads point to corresponding features). Serial reconstruction of this axon is shown in Figure 19. L, lateral. Scale bars = 100  $\mu\text{m}$  in A; 200  $\mu\text{m}$  in B,C; 50  $\mu\text{m}$  in D; 20  $\mu\text{m}$  in E.

lobe). The IPL, as shown by architectonic and connective studies (see, e.g., Pandya and Seltzer, 1982), encompasses multiple smaller areas. For ease of description, in this study we distinguish only between the posterior and anterior subregions, areas 7a and 7b, which are associated, respectively, with visual and somatosensory processes.

The technique of single axon reconstruction has been used extensively over the last 10 years in work from this and other laboratories (see, e.g., Saleem and Tanaka, 1996). However, it may be useful to recapitulate some of the key features of the procedure. An important first step, because extracellular injections result in the labeling of many thousands of axons, is the selection of individual processes ("pro-

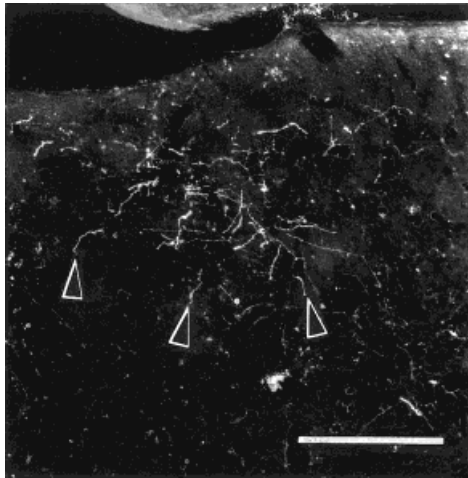


Fig. 6. Darkfield photomicrograph of terminations in the presubiculum anterogradely labeled by injections into ventromedial area TE [in the lateral bank of the occipitotemporal sulcus (OTS)]. Arrowheads point to some terminations. Scale bar = 100  $\mu$ m.

files”) for detailed analysis. Most efficient, in our experience, has been to identify well-isolated arbors in the gray matter and then to follow the axon trunk back into the white matter and toward its origin in the injection site. The selected profile is followed through sequential sections. This is accomplished first by matching at low magnification ( $\times 40$ ) a set of “landmarks,” blood vessels and 4–8 axon segments, possibly but not necessarily including the selected profile. Once the general region of interest is confirmed between neighboring slides, the matching process is repeated at higher magnification (typically  $\times 200$  or  $\times 400$  for gray matter and  $\times 100$  for white matter). Part of the matching process includes matching segments in the Z-dimension, at the top and bottom surfaces of the section. The segment of interest is drawn in, as well as the landmarks, and the process repeated for the next pair of adjoining slides. The set of landmarks is usually not constant over the course of the reconstruction, and the landmarks are not drawn in the final summary diagram.

Because serial section reconstruction is labor intensive, the sample size tends to be relatively small. Therefore, to achieve standardization, we prefer to concentrate on only two or three brains for the reconstructions. Features identified by this technique, however, to some extent, can be confirmed by reconstructions through shorter series and/or by scanning through individual sections; and additional brains in an experimental group are used for this purpose.

Two cases with injections of *Phaseolus vulgaris*-leucoagglutinin (PHA-L) into ventromedial area TE and area TF were used for comparison with the pattern of

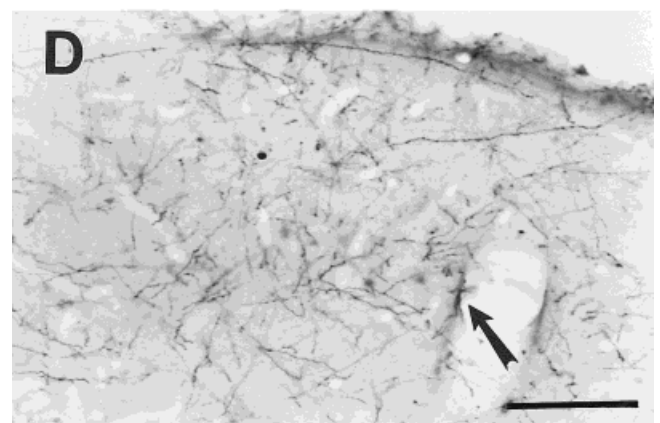
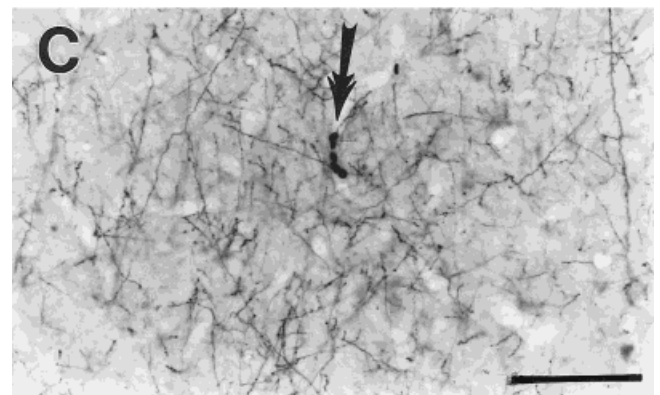
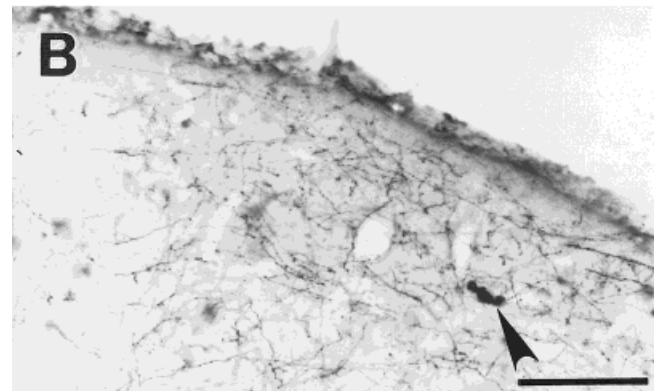
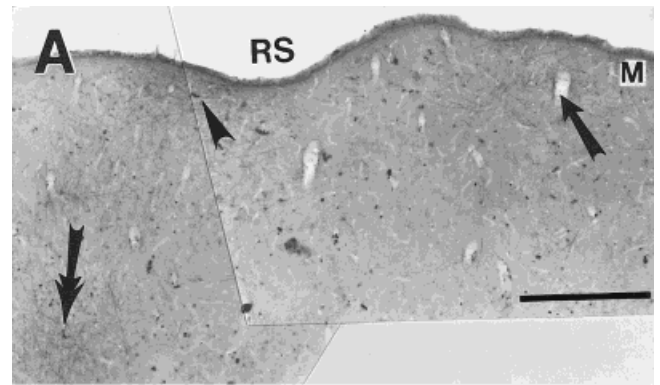


Fig. 7. Photomicrographs of terminations at the posterior tip of the RS labeled by injections into ventromedial area TE (in the lateral bank of the OTS). **A:** Low-magnification view of the border between the PRh (arrowhead) and ERh (single arrow) cortices. **B,C:** Higher magnification of label in the PRh cortex in the upper (arrowhead) and deeper (double arrow) layers. **D:** Higher magnification of label medially in the upper layers of the ERh cortex (arrows point to corresponding features in A and D). M, medial. Scale bars = 500  $\mu$ m in A; 100  $\mu$ m in B–D.

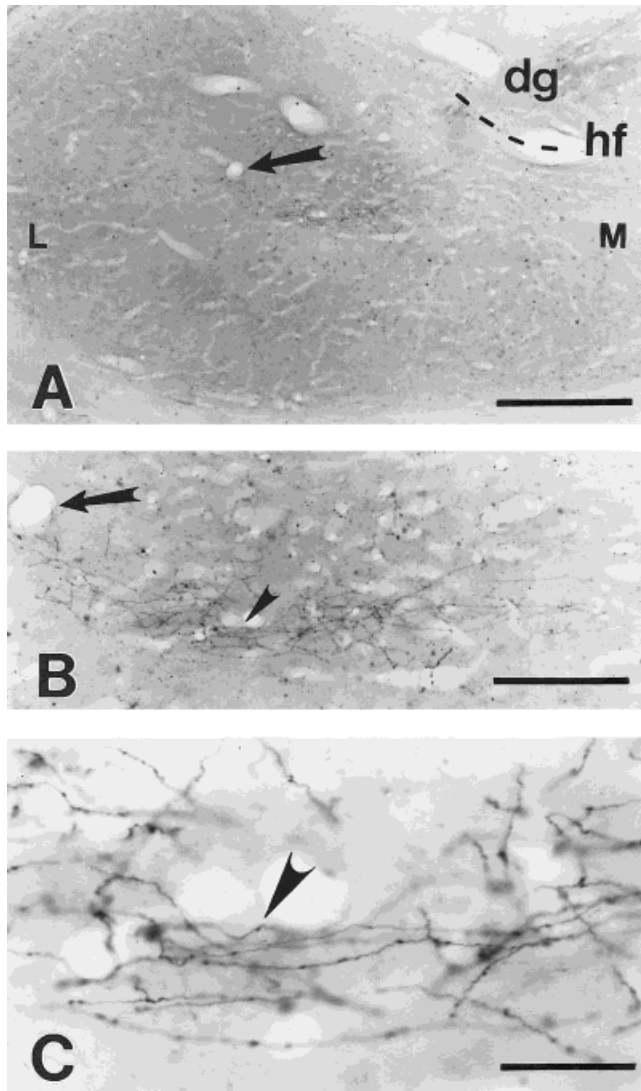


Fig. 8. Photomicrographs of terminations in area CA1 of the hippocampus anterogradely labeled by an injection in case 8. A–C are at progressively higher magnifications. Arrows in A and B and arrowheads in B and C point to corresponding features. dg, Dentate gyrus; hf, hippocampal fissure; M, medial; L, lateral. Scale bars = 500  $\mu\text{m}$  in A; 200  $\mu\text{m}$  in B; 50  $\mu\text{m}$  in C.

parietal connections to the presubiculum and associated fields. Some of the results from these cases have been reported in Wellman and Rockland (1997) and Rockland and Van Hoesen (1999). Several series of normal brains that were treated for parvalbumin, calbindin, or cytochrome oxidase (CO) were also consulted for architectonic features and boundaries. Preliminary results were presented in abstract form (Ding et al., 1999).

## RESULTS

### Laminar structure of the presubiculum

The presubiculum is a stripe-like periallocortical zone, about 2.0 mm wide  $\times$  6.0 mm long, immediately bordering the subiculum at the medial edge of the temporal lobe. It

is easily identified by staining for cell bodies, myelin, or various standard immunohistochemical markers (Fig. 2).

In Nissl stains (Fig. 2A), the presubiculum has four distinct strata:<sup>1</sup> a thin, cell-sparse layer (layer I); a broad, cell-dense layer (layers II–III); another cell-sparse zone (layer IV or lamina dissecans); and a deeper zone of more loosely packed neurons (layers V–VI). The superficial cell-dense layer is further divisible, with a thin outermost layer (layer II) of more tightly packed neurons. Layer I is about 150  $\mu\text{m}$  thick; layers II–III are about 400  $\mu\text{m}$  thick (including the outermost sublayer, which measures about 100  $\mu\text{m}$ ); and the deeper layers are about 500  $\mu\text{m}$  wide. Laminar dimensions, however, are highly variable, especially over the ML extent of the presubiculum. All of the layers are thinner at the lateral border with the subiculum and thicker at the medial edge, which usually wraps over the medial lip of the parahippocampal gyrus.

In tissue reacted for parvalbumin, there is a dense band of parvalbumin-positive neuropil and cell bodies corresponding to layers II–III. The calbindin pattern is slightly different and more complex. There is a dense, calbindin-positive plexus in layer I; a calbindin-poor band corresponding to the cell dense layer II of Nissl stains; and another band of calbindin-positive neuropil, with a few cell bodies, in layer III. Thus, the calbindin- and parvalbumin-positive bands are complementary in layers I (calbindin positive and parvalbumin negative) and II (calbindin negative and parvalbumin positive) but overlap in layer III (Fig. 2C–F). Many calbindin-positive fibers and a few parvalbumin-positive fibers are also discernible in the white matter below the presubiculum.

In addition to the main features of laminar organization, histochemistry for CO revealed sporadic patches, about 300  $\mu\text{m}$  wide, in layer I (Fig. 2G). The occurrence of patches varied between different animals and for the same animal across different AP levels of the presubiculum.

Layer I is further distinguished by a thick plexus of myelinated fibers (the reticular substance of Arnold; Gloor, 1997), which is especially prominent at posterior and middle levels of the presubiculum. These fibers may correspond to corticocortical connections, some of which have long preterminal portions in layer I (see below). Alternately or additionally, they may correspond to thalamic inputs from the anterior nucleus or pulvinar. No periodicity was discernible in myelin preparations (Fig. 2B).

### Global pattern of parietal projections to the presubiculum

In agreement with previous reports (Seltzer and Van Hoesen, 1979; Seltzer and Pandya, 1984; Selemon and Goldman-Rakic, 1988; Cavada and Goldman-Rakic, 1989), dense connections to the presubiculum were found from the middle and posterior subdivisions, but not from the more anterior subdivisions, of the IPL (area 7b; Table 1,

<sup>1</sup>In an alternate nomenclature (Lorente de No, 1934; Rosene and Van Hoesen, 1987), the superficial layers of the presubiculum (II and III) are termed the lamina principalis externa, and the deeper layers (V and VI) are called the lamina principalis interna. These are separated by the cell-poor lamina dissecans. This nomenclature, however, is less convenient for designating subdivisions within the superficial layers and, thus, has not been used in this report.

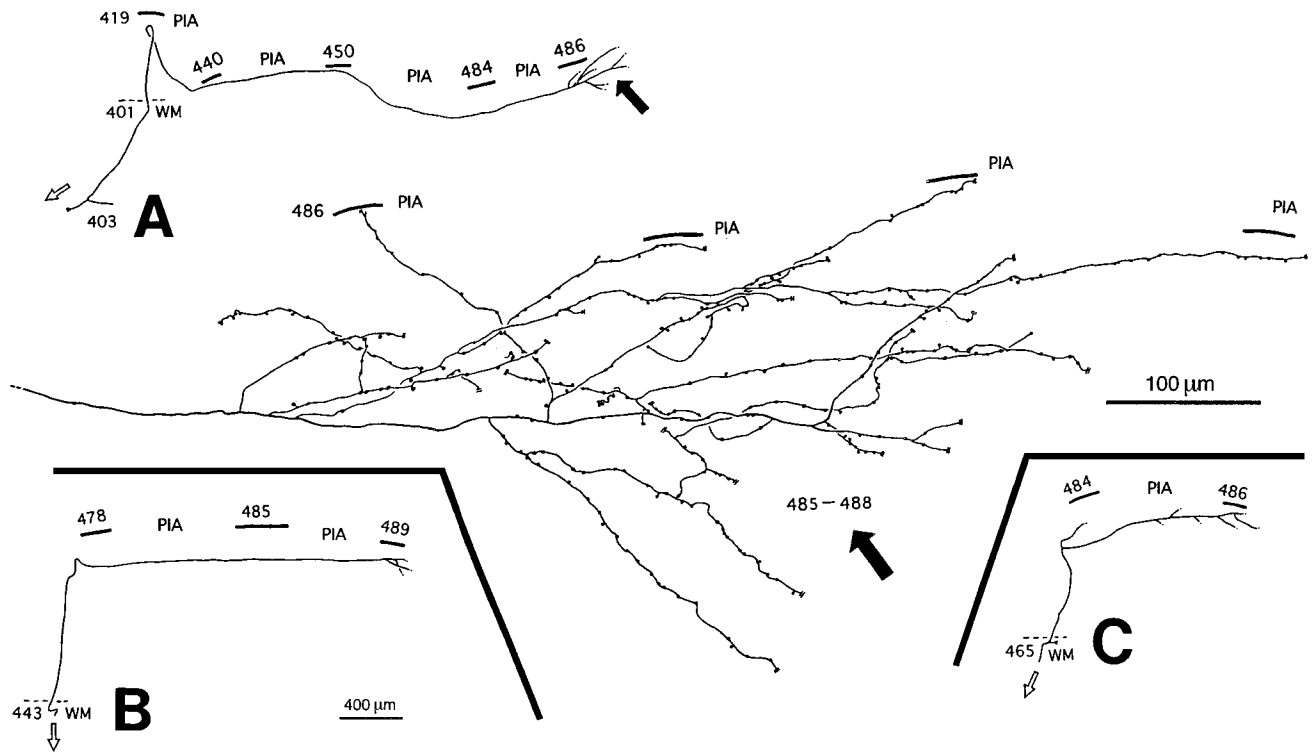


Fig. 9. Camera lucida reconstructions through serial sections of three axons with terminal arbors mainly in layer I of the presubiculum. These have been anterogradely labeled by injections of BDA into area 7a (case 5). **A–C**: Low-magnification views show overall configuration and extent. Reconstructions extend to fine terminal branches, which continued somewhat beyond what is actually shown. Higher magnification drawing is of distal portion from the axon shown in A. Arrows point to corresponding features (this axon is illustrated in Fig. 3D). Some of the distalmost portions may be incomplete (short double

lines). The hollow arrows in A–C mark the end point of the reconstruction and the proximal continuation of the axon toward the cell body. Numbers correspond to individual tissue sections [20 sections at 1.0-mm anteroposterior (AP) intervals]; larger numbers are progressively more anterior. PIA, pial surface of the brain; WM, white matter (at dashed lines). Conventions are the same in subsequent figures, except that, in some figures, the proximal continuation of the axon is marked with solid arrows.

Figs. 1, 3, 4). In the presubiculum, with our distribution of injection sites, connections were dense in the posterior one-third and moderate in its middle portion, with no projections to the anterior one-third. More anterior injections in the IPL tended to produce labeling in posterior regions of the presubiculum, and posterior injections resulted in terminations located more anteriorly.

At their most dense, projection foci tended to cover almost the whole ML extent of the presubiculum. In all cases, terminations concentrated in layers I and III, were somewhat less dense in layer II and were only sparsely distributed in the deeper layers (IV–VI). Terminations tended to have a bistratified distribution. In layers I–II, they frequently formed two to four patches about 0.15–0.30 mm across and separated by 0.4–0.6 mm from center to center (Fig. 4). These aligned in stripes over short distances ( $\approx 1.5$  mm AP); however, in reconstructions of serial sections, the stripes appeared to merge and fragment in an overall complicated pattern. Terminations in layer III often appeared patchy as well, but the pattern was less distinct than in layers I–II. Patches were not sharply delimited, as some terminations occurred in the interpatch spaces (Fig. 4). The superficial system of patches may correspond to or overlap with the pattern of CO staining, but further experiments with double labels

will be necessary to determine the exact relationship. In the medially adjoining parasubiculum (see Table 1), there were moderate projections from the five posterior injection sites (cases 5–9).

### Global connections to areas TE and TF

Regions around the occipitotemporal sulcus (OTS), as reported by other studies (Seltzer and Pandya, 1984; Cavada and Goldman-Rakic, 1989; Suzuki and Amaral, 1994a; Webster et al., 1994), received projections from all except the anteriormost injection (case 11). Terminations formed several foci in the lateral or medial banks of the OTS or medial to the sulcus. The medial foci correspond to area TF, as classically defined (Von Bonin and Bailey, 1947), and the lateral foci correspond to area TEO posteriorly or, more anteriorly, to a region characterized as ventromedial TE (Rockland and Van Hoesen, 1994; see also Felleman et al., 1997). In area TEO, terminations were mainly in layers I and VI; in the anterior areas, terminations in the dense core of the projection tended to be columnar.

### Global connections to the rhinal sulcus

All seven injections resulted in some terminations in the vicinity of the rhinal sulcus (RS); however, for the most

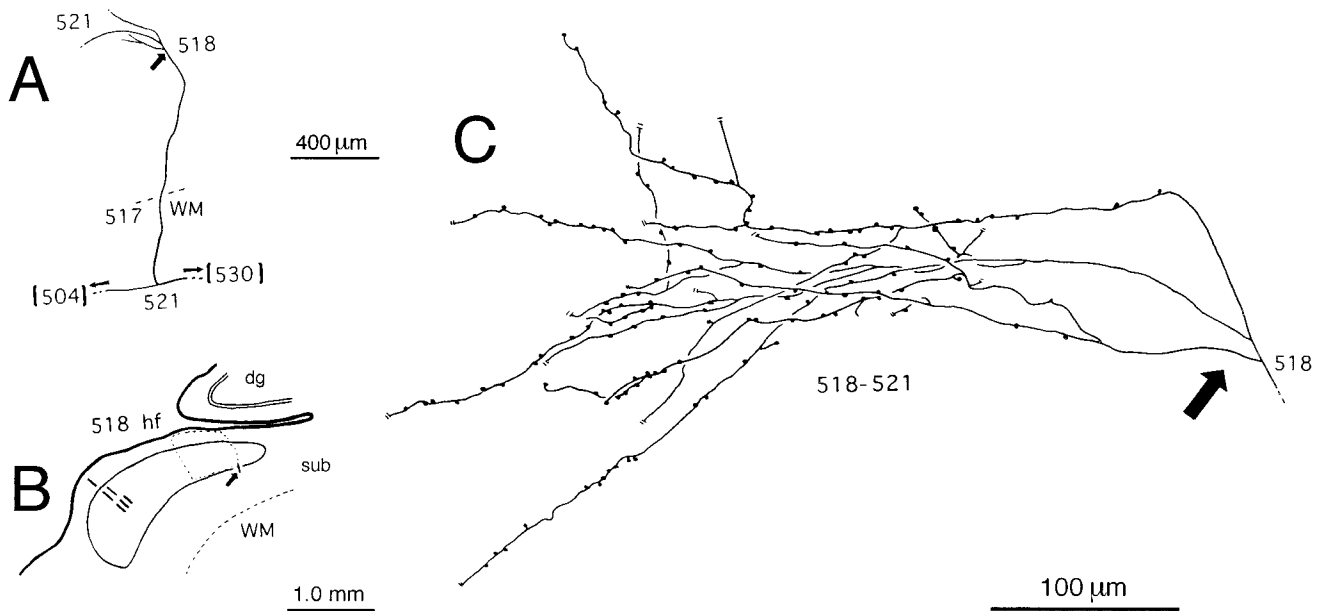


Fig. 10. Camera lucida reconstruction of axon 7-1 (case 7). **A:** Low-magnification schematic view showing that this axon terminates with a single arbor located within one of the projection patches. **B:** The patch is indicated by small dashed lines in this outline of section 518. **C:** Higher magnification detail of terminal specializations. Arrows in

A and C point to corresponding features; the arrow in B localizes the axon trunk in relation to the projection patch. The numbered arrows in A indicate how far the main axon was followed in both directions in the white matter. hf, Hippocampal fissure; dg, dentate gyrus; sub, subiculum.

anterior injection (case 11), these were very light (Table 1, Fig. 5). Despite the different locations of the injections within the IPL, most projections converged at a common locus, between the anterior OTS and the posterior tip of the RS and in the depth of the posterior RS (projections in case 10 extended somewhat more anterior). This is a complicated transition zone at the border between the perirhinal and entorhinal cortices that has been separately designated as the "prorhinal cortex" (Van Hoesen and Pandya, 1975). In recent studies (Amaral et al., 1987; Saleem and Tanaka, 1996), the medial bank of the RS has been included within the entorhinal cortex (EC). Terminations directly targeted this region, extending about 2.0 mm from the sulcal depth along both the lateral wall and the medial wall. In cases 7, 9, and 10, projections continued farther anterior in the RS and, at these levels, extended farther into the EC toward the medial lip of the RS.

Terminations in the medial bank of the RS occurred in layers I and II, with slight incursions into layer III. They did not appear to favor either the cell islands or the inter-island spaces, and portions of single axons could easily be observed in individual sections as branching to or crossing between more than one of the cell islands (Figs. 5, 19). Terminations in the lateral bank (perirhinal cortex) were denser in the deeper layers as well as the superficial layers.

### Contralateral connections to the presubiculum and RS

Five of the contralateral hemispheres were available for inspection (Table 1). Of these, the two most anterior injections (cases 9, 11) did not result in any detectable label in the presubiculum. Case 6, in which the injection site was posterior, had connections of moderate density in the

contralateral presubiculum (extending 0.35 mm AP). In case 7, with a larger injection situated in the middle portion of the IPL, the contralateral connections were more extensive (4.5 mm AP). Like the ipsilateral connections, these homotypical commissural terminations were concentrated in layers I–III. Sparse connections were observed in the contralateral parasubiculum (Table 1) in case 7 and (even sparser) in case 8.

In the contralateral RS, the more anterior cases (cases 9, 11), in which ipsilateral connections were relatively lighter, had no discernible terminations. Cases 6 and 8 had sparse projections, although these were less dense and less extensive than those on the side ipsilateral to the injections. Case 7 had abundant fibers in the white matter approaching the posterior EC (more anterior sections were not available; Table 1).

### Temporal connections to the presubiculum and RS

Of the two cases available with injections in temporal regions, ventromedial TE, but not TF, sent some projections to the presubiculum (Fig. 6). These were less extensive (<2.0 mm AP) and less dense than projections from parietal areas (contralateral hemispheres were not available).

Both temporal cases resulted in projections to the RS. Projections from ventromedial TE terminated mainly at the lateral border of the EC, extending about 2.0 mm into the medial bank (Fig. 7). This is the same border zone targeted by the projections from the IPL but is more anterior. Projections from area TF similarly targeted the lateral edge of the EC, but extended farther medially. The laminar pattern was similar to the parietal connections, except that it was denser in layer I.

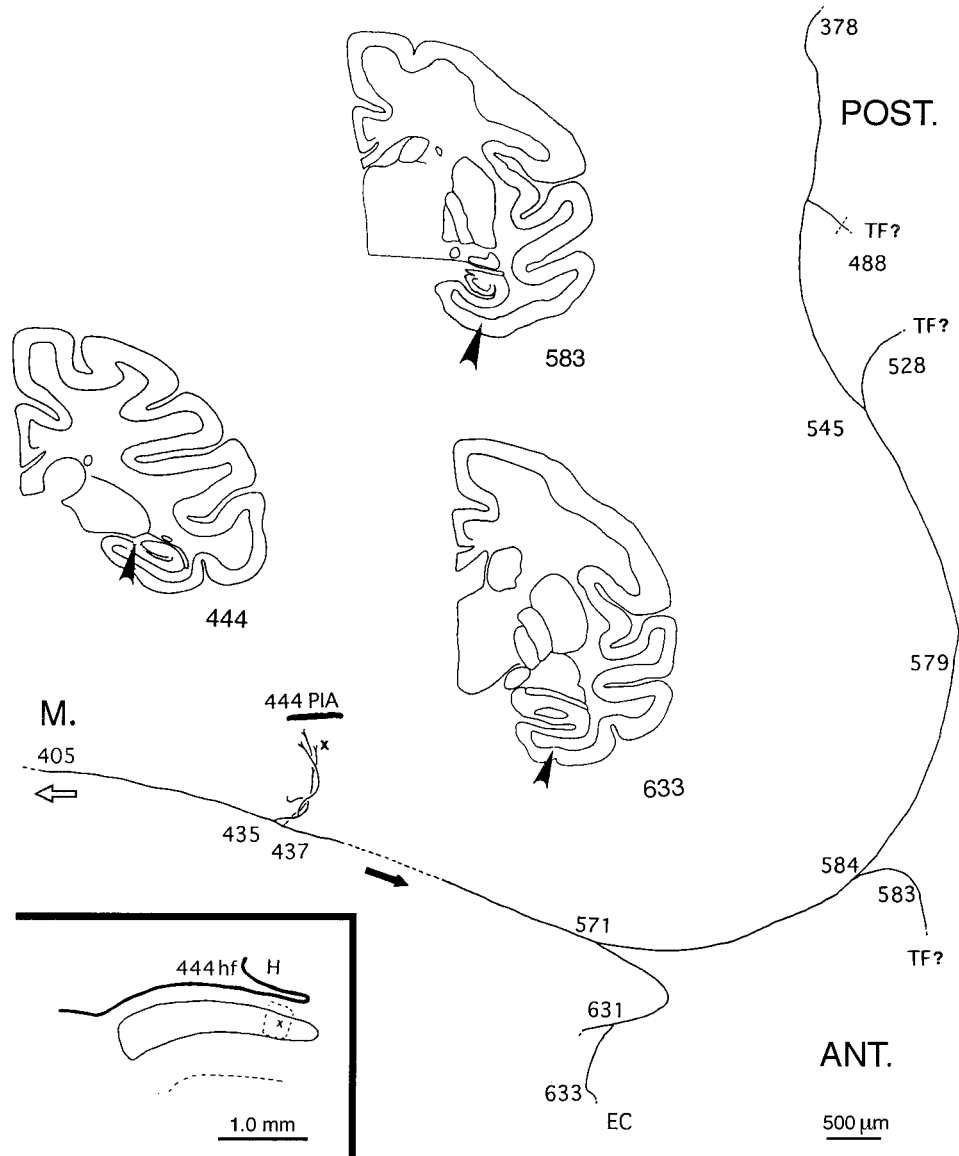


Fig. 11. Camera lucida reconstruction (through 255 sections) of axon 5-6. This axon also had a single arbor (marked by an x) that was traced into a projection patch (inset: x within the small dashed lines on the outline of section 444). The arbor was traced to its fine terminal branches, but the distalmost portions may be incomplete. This axon was traced from the white matter subjacent to the presubiculum (section 405). There is one terminal patch in the presubiculum (sections 435-444). The main axon, however, continues anteriorly, to projection foci at the lateral edge of the entorhinal cortex (EC; section 633) and area TF. (The middle portion of the white matter trajectory

has been compressed for the sake of space; dashed lines and arrow.) There are three separate terminations to area TF medial to the OTS (at sections 583, 528, and 488). These constitute a posterior loop of the axon that continues at least another 5.5 mm posterior (to section 378) in the vicinity of the OTS. The fine distal portion of the axon was lost in the white matter at section 378. (The segments at sections 378-584 are approximately in the same location in an AP slab.) The positions of portions of the axon at different AP levels are indicated by arrowheads on the three (coronal) section outlines. M, medial; Post, posterior; Ant, anterior.

**Connections to CA1**

On the basis of three of these cases (cases 5, 7, and 9), direct connections had been previously reported from the IPL to CA1 (Rockland and Van Hoesen, 1999). Direct connections to CA1 were also found in three of the additional four cases reported here (Table 1, Fig. 8). Connections were most dense in cases with more posterior injections (in area 7a). In case 11 (situated in area 7b) and case

10 (anterior in area 7a), terminations were very light and were restricted to the most posterior part of CA1.

**Single axons terminating in layer I of the presubiculum**

Long axon fragments (>0.5 mm) could easily be found in layer I in single sections (Fig. 3). The finding that some axons target exclusively layer I was more precisely dem-

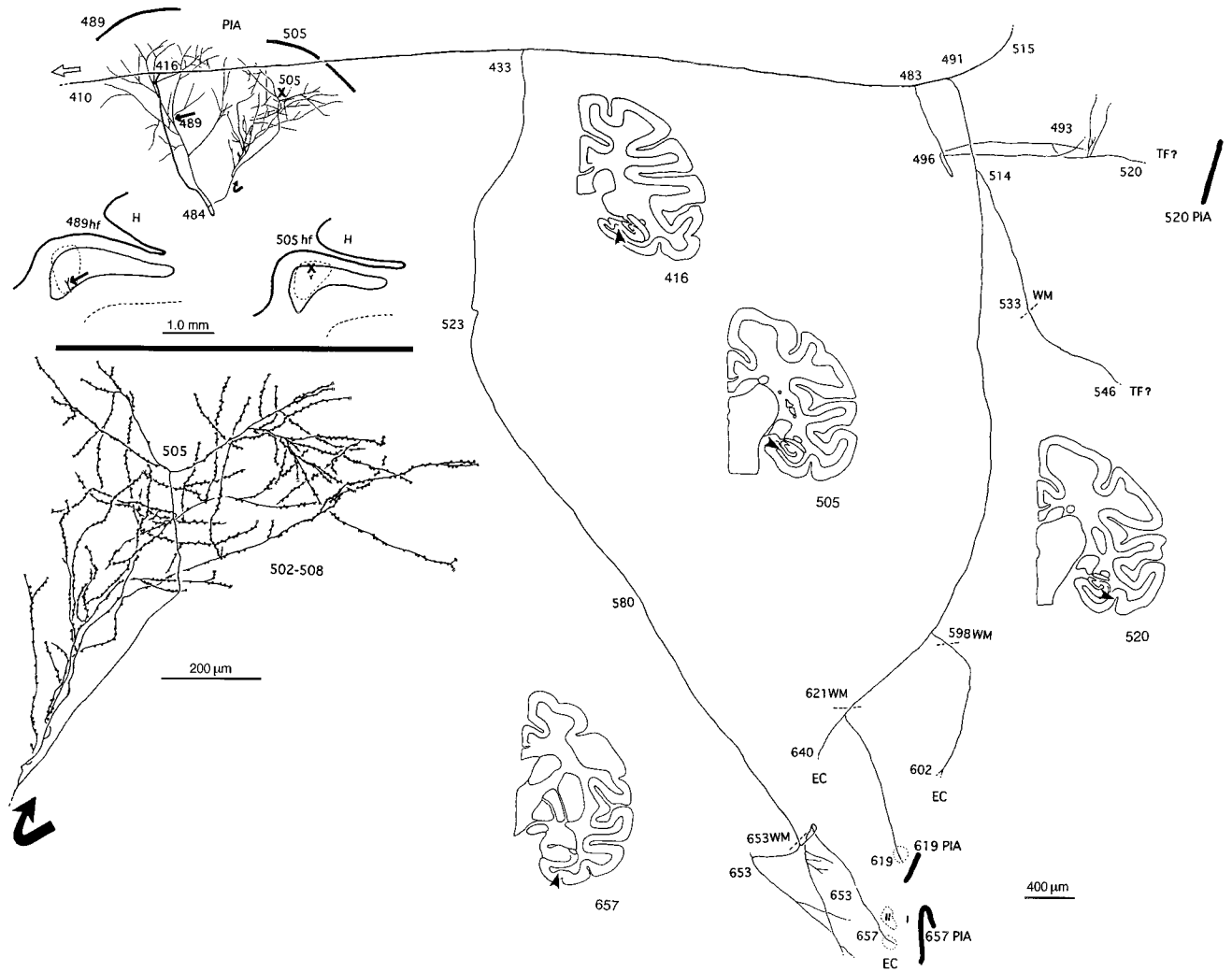


Fig. 12. Camera lucida reconstruction (through 247 sections) of axon 5-3. This axon has two arbors slightly offset from each other in the AP plane. Both seem to target the same projection patch, as indicated by the straight arrow and the x within the dashed lines on the outlines of sections 489 and 505. The more lateral arbor is redrawn at higher magnification to show details of terminal specializations (curved arrows point to corresponding features at lower and higher magnifications). Like axon 5-6, this axon continues anteriorly

to projection foci in the EC (sections 602, 619, 653, and 657) and in what is probably area TF (sections 493, 520, and 546). A third branch (section 515) was lost in the vicinity of area TF and may have continued posteriorly. The positions of portions of the axon at different AP levels are indicated by arrowheads on the four section outlines. Note the twisted geometry in the presubiculum, where the arbors recur toward the surface after descending from the main axon at section 416.

onstrated by serial reconstruction of four axons (case 5), three of which are shown in Figure 9. The total lengths of these axons in layer I were 1.2 mm, 2.0 mm, and 3.0 mm. Some boutons were scattered along the full portion of the axon in layer I, but most were concentrated at the distal 0.5–0.7 mm.

**Single axons terminating in the presubiculum with simple arbors**

Other axons gave rise to simple arborizations, which extended into layers I–III of the presubiculum. Five of these axons were reconstructed, three of which are shown in Figures 10–12. For axon 7-1, there was a single arbor at least 0.4–0.5 mm wide (fine, distalmost portions were lost in a patch of dense terminations) (Fig. 10).

Axon 5-6 also had a single projection focus in the presubiculum. For this axon, like 7-1, after giving off terminations in the presubiculum, the main axon continued ventral and lateral in the white matter. Three branches were followed to projection foci in a region in the medial bank of the OTS that probably corresponds to area TF. A fourth anterior branch was followed to the border of entorhinal and perirhinal cortices (Fig. 11).

Axon 5-3 had two separate arbors, one lateral and slightly anterior to the other. Both had terminations in layers I–III (Fig. 12). The medial arbor measured about 0.8 mm ML × 0.9 mm AP, and the lateral arbor (at the curved arrow in Fig. 12) measured 0.8 mm ML × 0.3 mm AP. This axon in addition sent branches to three foci in area TF (separated by intervals of 1.0–1.5 mm) and three

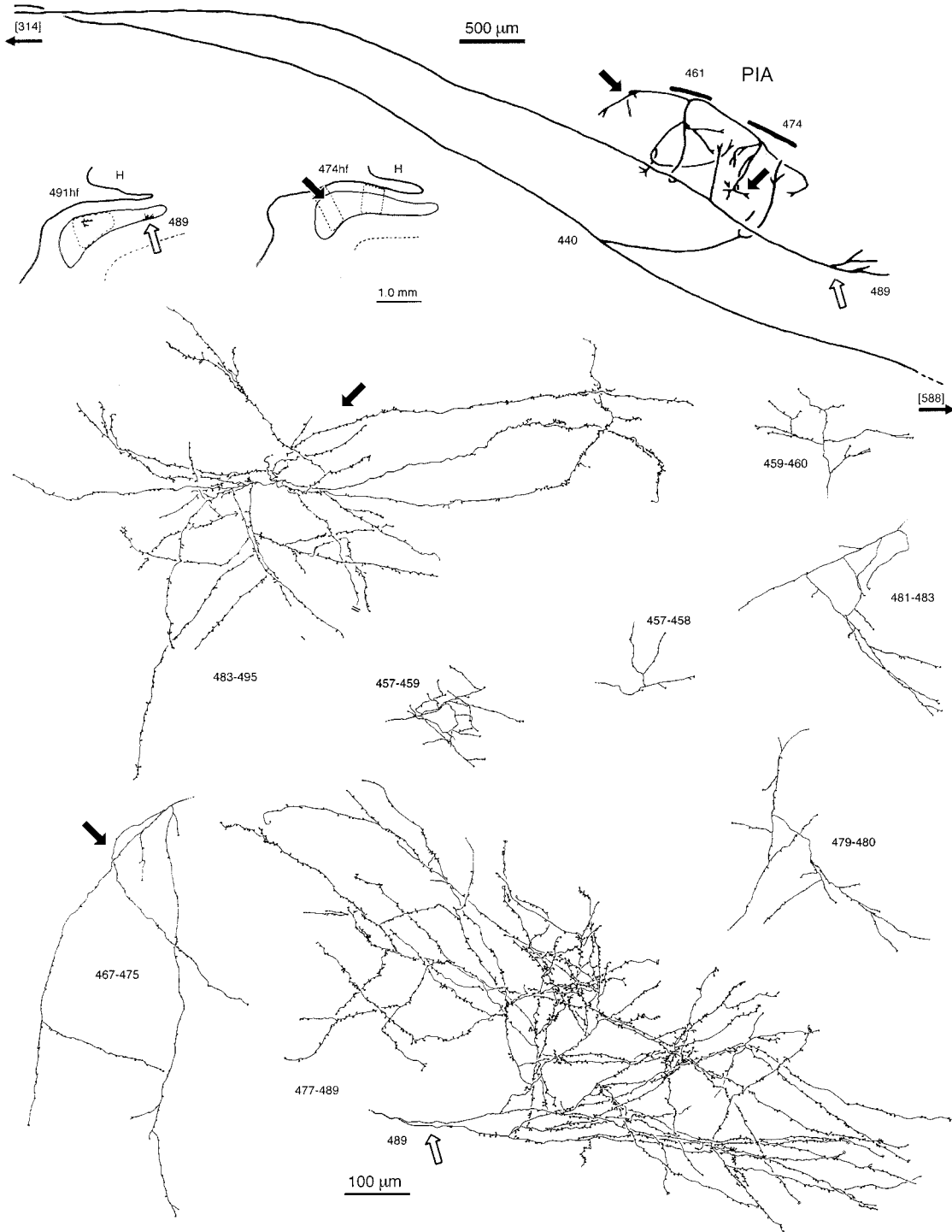


Fig. 13. Camera lucida reconstruction (through 261 sections) of axon 5-2 with a complex arborization extending over a large mediolateral extent of the presubiculum. This consists of two large arbors (redrawn at higher magnification at the open arrow and the left-pointing arrow); a smaller, medially located arbor (at the right-pointing arrow) and five partially overlapping, smaller arbors (unmarked; see also the photomicrographs in Fig. 15C–E). Each of these

arbors was associated with a denser projection patch, as indicated by the icons within the small dashed lines on the outlines of sections 474, 489, and 491. Note that several of the arbors descend from more superficial branches into the deeper layers. This axon continues in the white matter beyond the presubiculum (and was followed through section 588). The proximal portion of this axon was followed to section 314 (arrow).

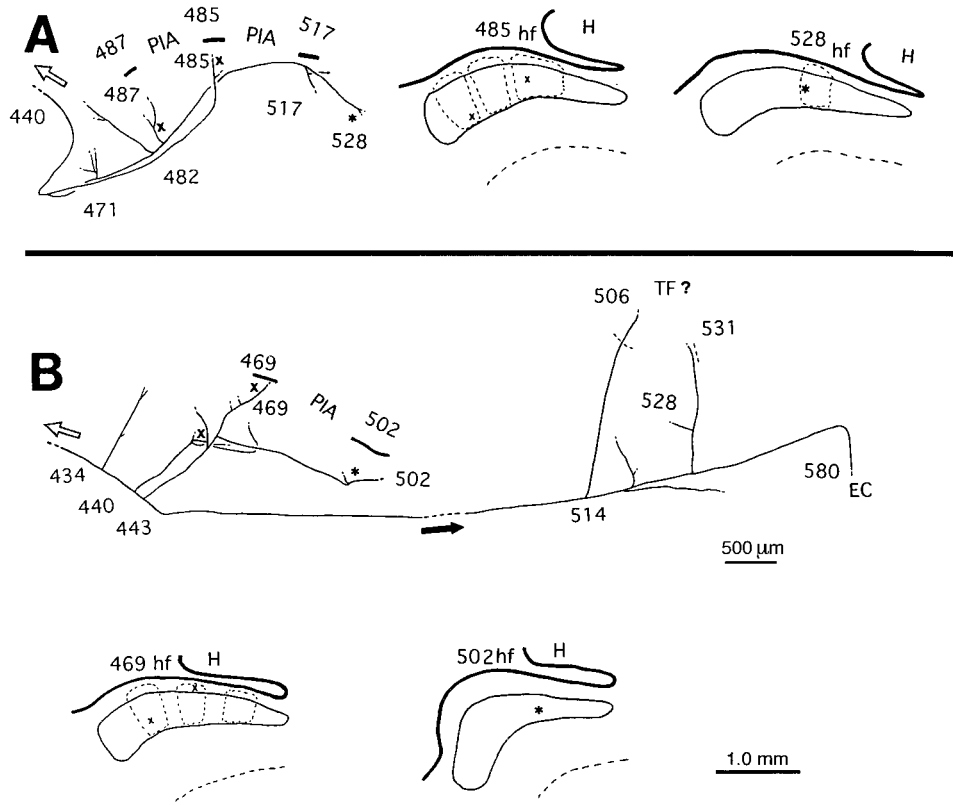


Fig. 14. Partial reconstructions of axons 7-4 (A) and 7-5 (B). Each of these has multiple arbors that were followed into a projection patch (x within the small dashed lines on the outlines of sections 485 and 528 (axon 4) and sections 469 and 502 (axon 5). Axon 4 appeared to terminate exclusively within the presubiculum, and axon 5 continued

beyond, to projection foci at the lateral border of the EC and to what is probably area TF. (To save space, the white matter trajectory of axon 5 has been compressed, as indicated by the dashed lines and arrow.)

foci at the lateral edge of the EC (separated by intervals of 1.0 mm: at sections 602, 619, 640, and 657). Within these foci, the actual terminations were either too fine to trace (in the EC) or were lost in a field of dense terminations (in area TF).

**Single axons terminating in the presubiculum with complex arborizations**

Five axons were documented with multifocal, more complex arborizations, of which three are illustrated and described below: Axon 5-2 had two large arbors (1.0 mm ML × 0.7 mm AP and 0.6 mm ML × 0.6 mm AP) and multiple smaller arbors (Fig. 13). Terminations were in layers I-III. Five smaller arbors partially overlapped in two projection patches that were separated by 1.0 mm AP (sections 457-460 and 479-483). A sixth arbor was situated about 0.8 mm laterally. Overall, the arbors contributed to four patches distributed over 2.4 mm ML × 1.5 mm AP. Beyond the presubiculum, the axon trunk continued ventrally and laterally to the white matter below area TF.

Axon 7-4 had five distinct branches that partially converged in three termination patches distributed over 1.5 mm ML × 2.0 mm AP. This axon did not send collaterals beyond the presubiculum (Fig. 14A).

Axon 7-5 had multiple branches directed to three termination patches spaced over 1.0 mm ML × 1.5 mm AP

(terminations for the medialmost branch could not be followed). Collaterals were traced to several foci in area TF and to the lateral edge of the EC (Fig. 14B).

In addition to the more complete reconstructions described above, measurements were made of six, partially reconstructed single arbors from cases 5, 8, and 10 (Fig. 15). These ranged from 0.4 mm to 0.5 mm in the longest dimension.

**Single axons terminating in the contralateral presubiculum**

Of six axons that were analyzed in the contralateral hemisphere from case 7, four had simple arborizations, of which three are illustrated (Figs. 16-18). Arbors were concentrated in layers I-III. Two of these axons (C1 and C2) had a single arbor. One measured 0.6 mm ML × 0.8 mm AP, and the other measured about 0.6 mm in diameter (Fig. 16).

Axon C-3 had three arbors, all targeting one projection patch. There was one large, principal arbor (about 0.6 mm in diameter; straight arrows in Fig. 17); a small extension (≈0.2 mm in diameter); and a second small arbor (0.2 mm in diameter; curved arrow in Fig. 17). The second arbor was offset from the main cluster by an interval of about 1.0 mm.

Axon C-4 had a complex arborization. There was one principal arbor (X at 355 in Fig. 18) and several other branches

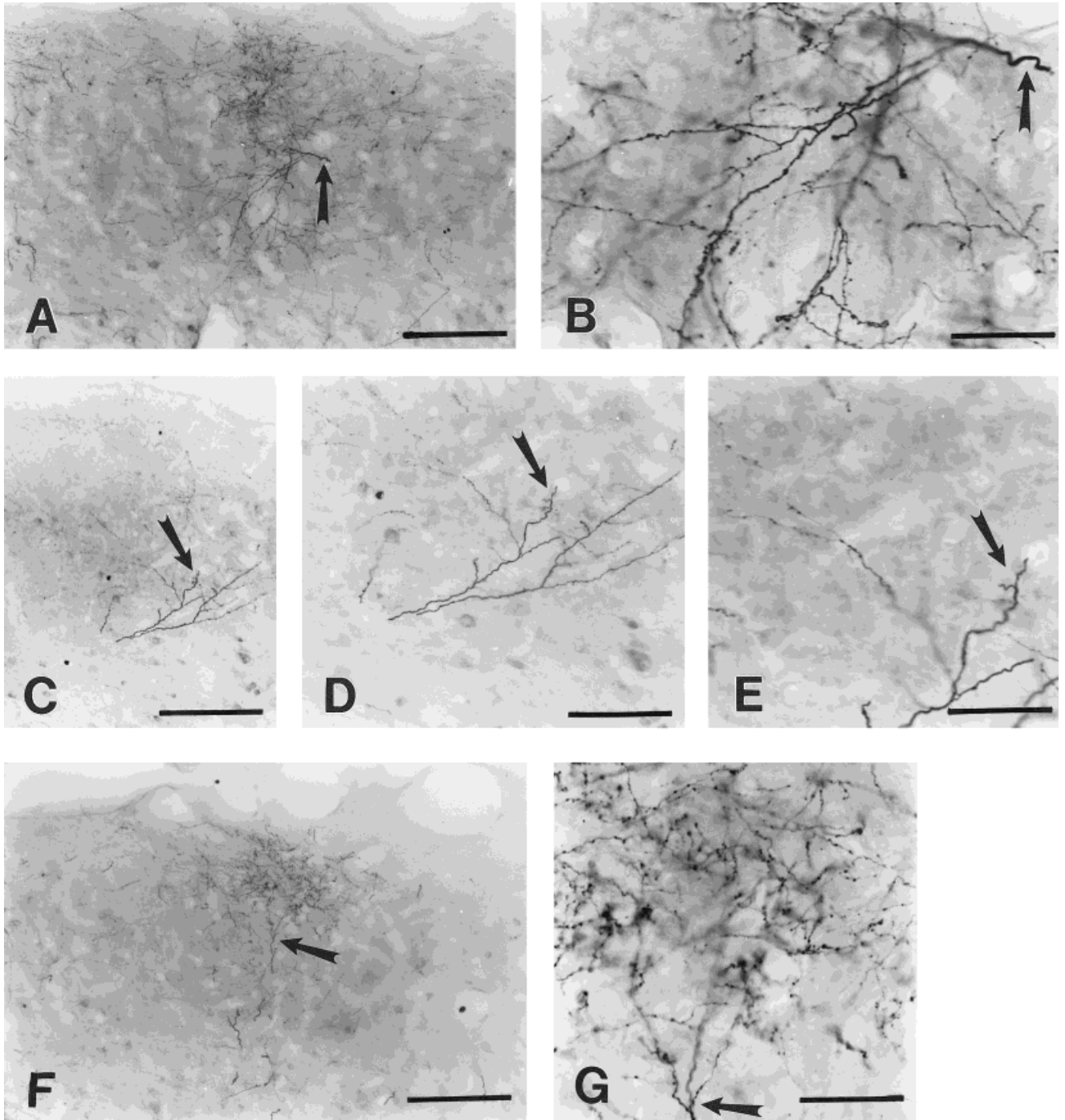


Fig. 15. Photomicrographs from case 5 of portions of single BDA-labeled arbors in the presubiculum. **A:** Arbor terminating in layer III. **B:** Higher magnification of the area indicated by the arrow in A. **C:** Arbor terminating in layers II–III. This arbor is part of an axon that is illustrated more fully in Figure 13 (at the open arrow). **D,E:**

Progressively higher magnifications of the area indicated by the arrow in C (D) and D (E). **F:** Arbor terminating in layers I–II. **G:** Higher magnification of the area indicated by the arrow in F. Scale bars = 200  $\mu\text{m}$  in A,C,F; 100  $\mu\text{m}$  in D; 50  $\mu\text{m}$  in B,E,G.

that converged in a second focus. The two foci were separated by 1.2 mm ML but were at about the same AP plane.

Of these six axons, axons C-1 and C-4 (and one that is not illustrated) had collaterals that clearly continued in

the white matter beyond the presubiculum. Axons C-1 and C-3 were followed only a short distance into the white matter, and the presence or absence of collaterals could not be ascertained.

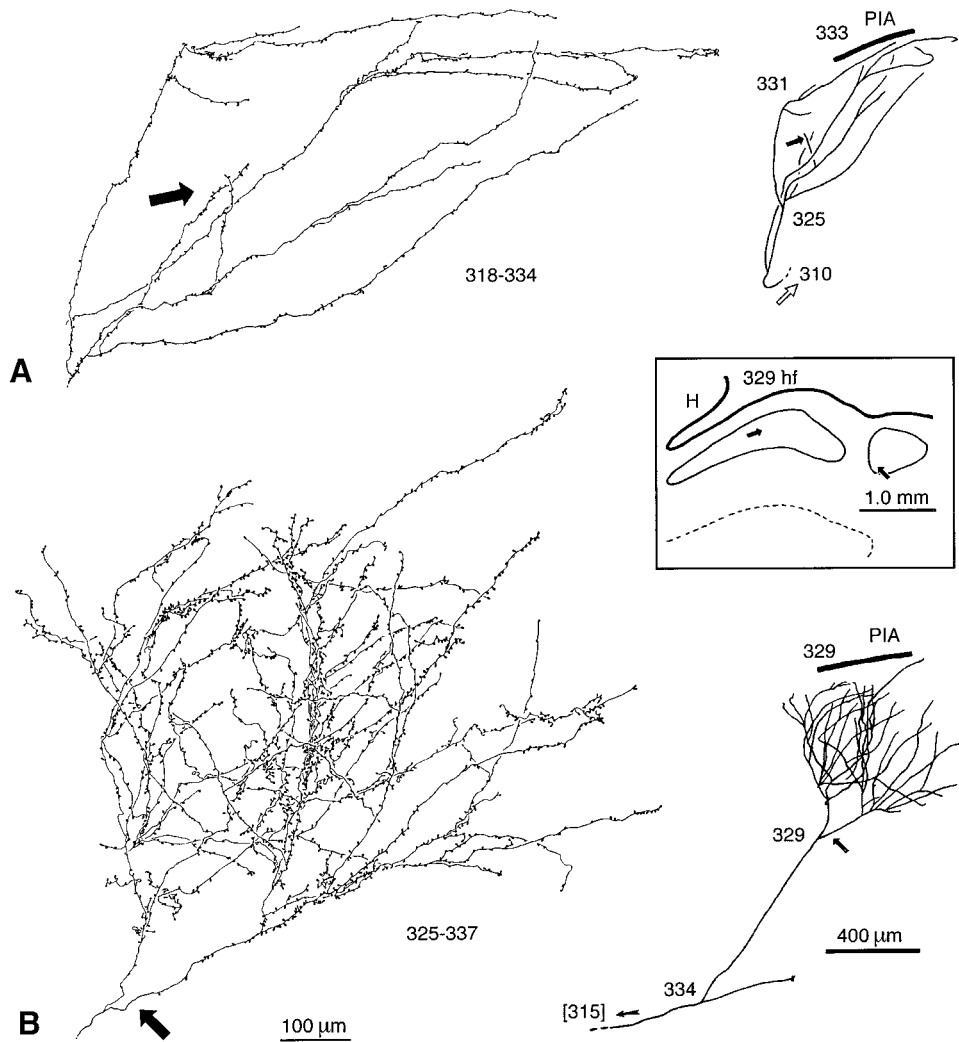


Fig. 16. Camera lucida reconstruction of axon C-1 (A) and axon C-2 (B) terminating in the pre- and parasubiculum contralateral to the injection site. Both of these axons have what appears to be a single arborization [measuring about 0.6 mm mediolateral (ML)  $\times$  0.8 mm AP, and 0.6 mm ML  $\times$  0.6 mm AP, respectively]. Arrows point to

corresponding features at low and high magnification. Arrows within the outlines of section 329 indicate the approximate position of these two axons. Axon C2 continued in the white matter beyond the presubiculum (followed to section 315).

### Single axons terminating in RS

One axon (from case 9) was partially reconstructed at its distal termination at the lateral border of the EC. There were two partially overlapping arbors, about 0.30 mm and 0.45 mm wide each (Figs. 5C, 19). Together, these arbors extended over four cell islands in layer II with some incursion, medially, in the subjacent layer III. Terminations occurred in both the cell islands and the interisland spaces and also deeper in layer III along the ascending portion of the axon. A total of 263 boutons were counted along this segment. Two other single arbors (cases 9 and 10) were partially reconstructed and were found to measure about 0.30 mm wide.

### Axon caliber and bouton counts

Observations were made on labeled axon segments in the white matter below the presubiculum. These varied in diameter. Most were about 1.0  $\mu$ m wide, a few were

large (2.0–3.0  $\mu$ m wide), and many appeared to be <1.0  $\mu$ m.

Axon 5-2 had a total of 2,668 boutons (738 and 1,559 in the two large arbors and 371 among the six smaller arbors). Of the three contralateral arbors illustrated, axon C-1 had at least 400 boutons, axon C-2 had 1,545 boutons, and axon C-3 had 931 boutons. Bouton numbers in layers I–II were difficult to assess because of the overall density of the label. These numbers might be somewhat low because of the possibility of further fine distal extensions. Boutons were a mix of stalked (terminaux) and beaded (en passant) and were not qualitatively distinguishable from typical corticocortical terminations.

### DISCUSSION

Connections to the presubiculum from area 7a of the IPL have been reported in previous studies using other

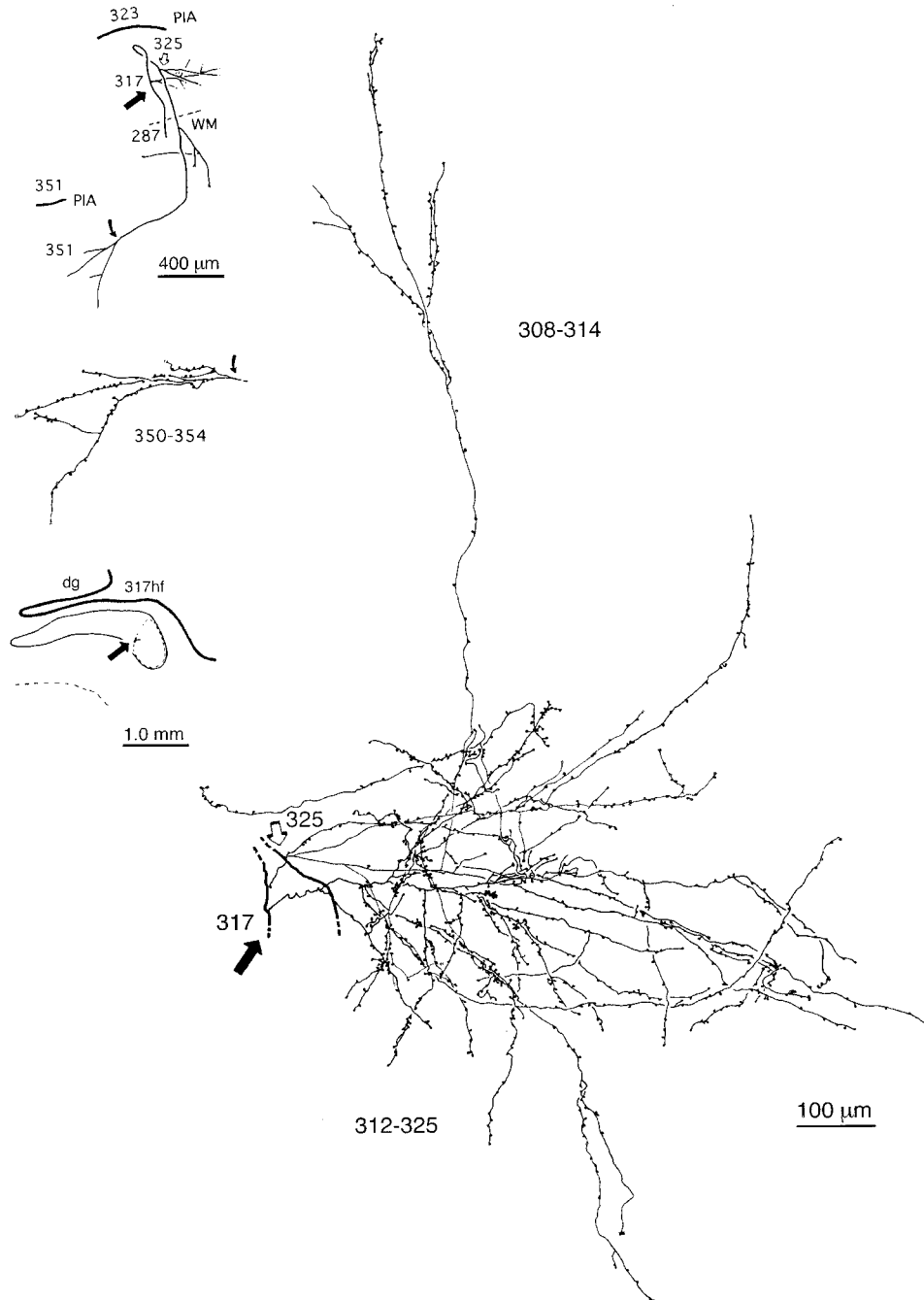


Fig. 17. Camera lucida reconstruction of axon C-3 (case 7) terminating in the presubiculum contralateral to the injection site. This axon has one large arbor (about 0.6 mm in diameter; solid straight arrow) and a smaller arbor (solid curved arrow). These are offset by about 1.0 mm AP and 1.0 mm ML. The larger arbor itself has two

partially overlapping components (open arrow) and a small posterior extension. The position of the axon is indicated at one AP level by the solid straight arrow and the small dashed lines on the outline of section 317. These represent a dense projection patch.

techniques (Seltzer and Van Hoesen, 1979; Seltzer and Pandya, 1984; Cavada and Goldman-Rakic, 1989). By using single axon reconstruction, the present work further demonstrates that 1) individual arbors terminating in the presubiculum are relatively large, and 2) individual axons commonly send branches to other targets in the parahip-

pocampal region (area TF, perirhinal cortex, and entorhinal cortex) in addition to the presubiculum. These findings are discussed in relation to the functional architecture of the presubiculum and their possible implications for multiple memory systems associated with the temporal lobe.

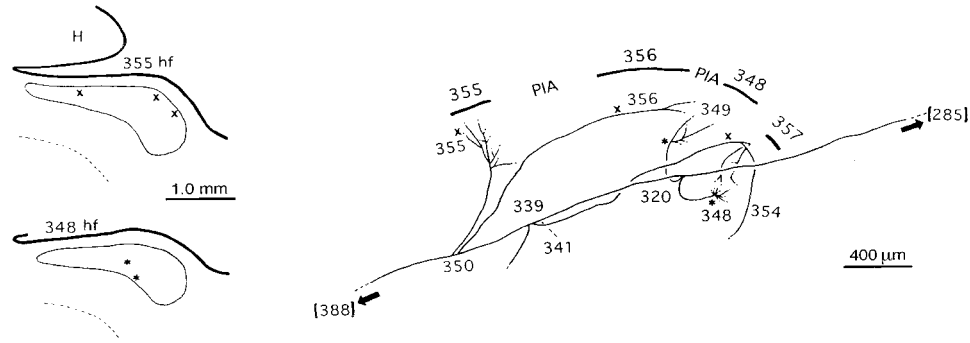


Fig. 18. Camera lucida reconstruction of axon C-4 terminating in the presubiculum contralateral to the injection site. This axon has a complex arborization consisting of a solitary large arbor situated laterally (x at 355) and multiple branches that partially converged in

two projection patches situated more medially. The location of the arbors within projection patches is indicated by icons on the outlines of sections 348 and 355. The main axon continued in the white matter beyond the presubiculum (followed to section 285).

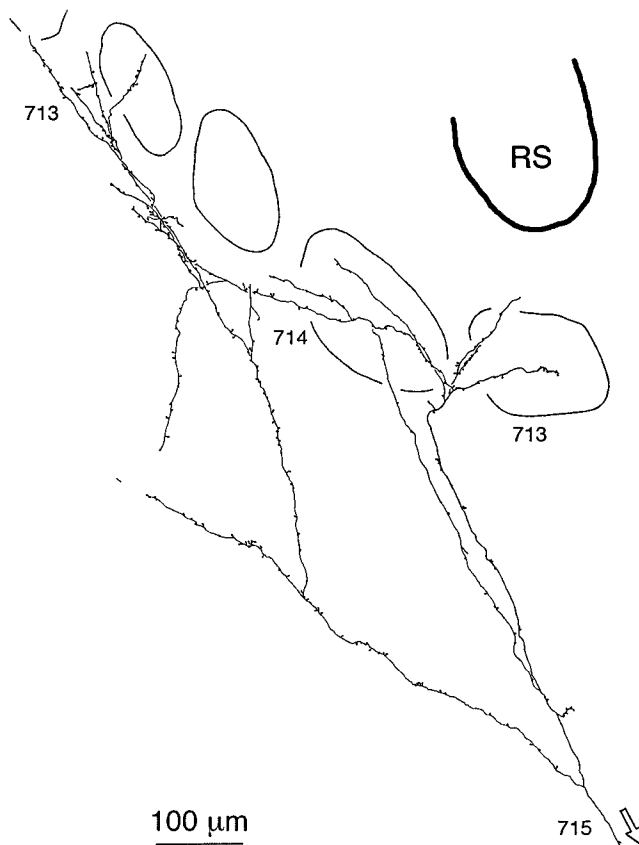


Fig. 19. Camera lucida reconstruction of an axon (from case 9; sections 712–715) terminating at the lateral border of the EC (see also Fig 5C–E). There are two small arbors (about 0.30 mm and 0.45 mm in diameter) that terminate in the vicinity of the cell islands in layer II. Terminal specializations extend between and beyond the islands. RS, rhinal sulcus.

### Configuration of individual arbors

There are still relatively few reports about corticocortical connections at the level of single axons. The available evidence suggests that, with the exception of feedback and

other inputs to layer I, individual arbors tend to be  $\leq 0.3$  mm in diameter; for example, terminations from area TE to perirhinal cortex (Saleem and Tanaka, 1996) and terminations from several visual cortical areas (summarized in Rockland, 1997). By comparison, terminations from the IPL to the presubiculum cover larger territories (0.3–0.8 mm) either as single or multiple arbors (Fig. 20). Given the narrow width of the presubiculum, the large terminal fields are even more substantial. Possibly, the size of IPL arbors may be less related to their termination in the presubiculum than to their origin in the IPL; but preliminary results indicate that arbors terminating in area TF are  $\leq 0.3$  mm in size. This observation is consistent with what appears to be a trend associated with limbic-type fields. That is, other studies have reported divergent connections within both the hippocampal (Sik et al., 1993) and entorhinal (Tamamaki and Nojyo, 1993; Wellman and Rockland, 1997) pathways.

Another system of divergent terminations that may serve as a useful comparison is the subpopulation of magnocellular connections from the lateral geniculate nucleus to the primary visual cortex. These axons have large arbors (0.3–0.5 mm  $\times$  0.6–1.2 mm), large numbers of boutons ( $>3,200$ ), and contact large numbers of postsynaptic neurons (Blasdel and Lund, 1983; Freund et al., 1989). In the case of magnocellular axons, these features correlate with high temporal sensitivity and a role in motion detection. In the case of the presubiculum, large terminal fields, which presumably contact large postsynaptic populations, might be consistent with a posited involvement of this structure in visuospatial functions, such as path integration or navigation (see, e.g., Robertson et al., 1999).

Some axons from the IPL selectively target layer I, where they can extend for distances of 1.0–3.0 mm. This pattern is reminiscent of “feedback” connections in the early sensory pathways. Like sensory feedback connections, layer I terminations might originate from neurons in layer 6 and may well be a distinct subpopulation. Whether they are functionally similar to “classical” feedback connections is less apparent (for further discussion of problems in classification resulting from overreliance on laminar patterns, see Wellman and Rockland, 1997).

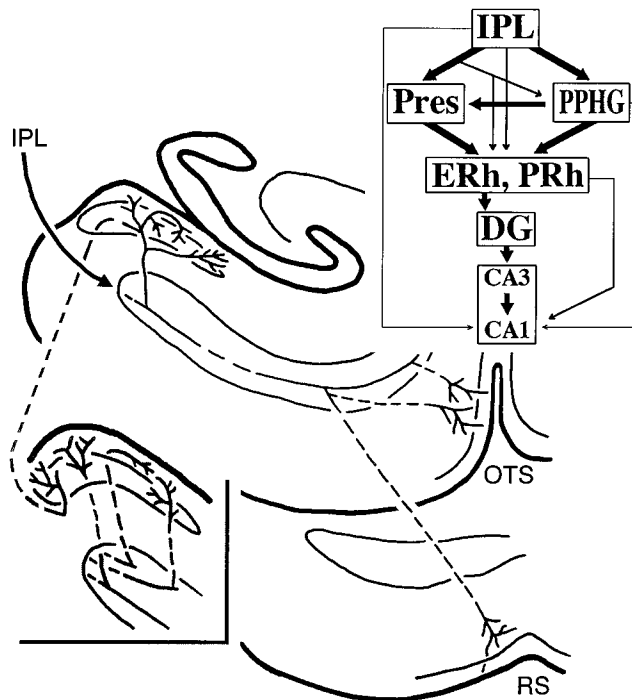


Fig. 20. Schematic diagram summarizing the different configurations of IPL axons terminating in the presubiculum (Pres). The summary also shows their branching to the perirhinal/entorhinal border (ERh, PRh) and to areas around the OTS. The arrow-and-block diagram on the right illustrates some of the multiple routes, direct and indirect, connecting the IPL to different stages in the corticohippocampal pathway. The thinner lines indicate sparser connections. PPHG, posterior parahippocampal gyrus. (Contralateral and subcortical connections are not shown.)

### Banding pattern of terminations

Goldman-Rakic et al. (1984), in their earlier autoradiographic study of prefrontal connections, noted that terminations to the presubiculum form discrete bands, 250–400  $\mu\text{m}$  wide, in the cell-sparse layer I. Our material also indicated a disjunctive pattern of terminations in layer I, but the precise organization was difficult to ascertain and also seemed somewhat variable among the different brains. Most frequently, there were three to four discrete terminal patches, 300–500  $\mu\text{m}$  across, in layer I and the upper part of layer II. These aligned in a stripe-like pattern over short distances (0.5–1.5 mm AP); however, over larger distances, they appeared to merge and fragment in a more complicated pattern, perhaps resembling the striosomes of the caudate nucleus. In some animals, the terminations formed two clearly separate strata, with a second zone of patchy terminations in layer III.

The superficial termination patches may be indicators of an underlying functional compartmentalization. This possibility is supported by the patchy distribution of other markers: CO (present report) and somatostatin (Bakst et al., 1985).

Our results further emphasize the laminar complexity of the presubiculum, especially in its most superficial strata (layers I and II), where the afferent terminations commonly form a bistratified pattern. This laminar com-

plexity is corroborated by the pattern of calbindin and parvalbumin staining. Immunohistochemistry for these markers shows that plexuses coincide in layer III but are complementary in layers I and II.

### Single axons branch to the presubiculum, area TF, and the rhinal sulcus

Connections from the IPL target several fields within the medial temporal lobe that are mutually interconnected and functionally related as part of the hippocampal memory system (Van Hoesen and Pandya, 1975; Kosel et al., 1982; Amaral et al., 1984; Insausti et al., 1987; Suzuki and Amaral, 1994b). In addition to the presubiculum, these structures include area TF and the perirhinal and entorhinal cortices (Van Hoesen et al., 1972; Seltzer and Van Hoesen, 1979; Seltzer and Pandya, 1984; Cavada and Goldman-Rakic, 1989; Andersen et al., 1990; this report).

These areas are commonly viewed as progressive stages in the main corticohippocampal pathway. It was therefore unexpected to discover that 10 of 14 axons terminating in the ipsilateral presubiculum also send branches to several of these cortical areas. For four of these axons, branches were specifically identified to area TF in the vicinity of the OTS, and to bordering regions of the perirhinal and entorhinal cortices.

Collateral projections have been identified in other cortical systems (for reviews, see Bullier and Kennedy, 1987; Rockland, 1997). In the early visual pathways, some neurons in area V1 project to both V2 and V4, and some neurons in V2 project to both V4 and TEO (Nakamura et al., 1993). Some feedback projections from temporal areas have collaterals to multiple visual areas, including areas V1 and V2 (Kennedy and Bullier, 1985; Rockland and Van Hoesen, 1994; Rockland et al., 1994; Rockland and Drash, 1996). In these instances, the collateralized projections are a subset estimated as <20% of the total projection. This is considerably lower than the proportion of collateralized axons we found for parietopresubicular projections (70%). In both systems, however, the amount of collateralization is higher than what has been reported ( $\approx 1\%$ ) after injections of multiple retrograde tracers into various subdivisions of orbitofrontal cortex (Barbas, 1995).

A logical question is whether a high degree of collateralization might be a particular feature of memory-related systems. In this regard, it will be important to determine whether the proportion of branched axons reported in this study is representative or whether there may be a possible sampling bias, in which case, this proportion in fact may apply only to a particular subpopulation. Another important question is whether other cortical connections to the presubiculum are heavily collateralized; for example, prefrontal connections from areas 9 and 46, which project to the same medial temporal areas as the IPL (area TF, perirhinal and entorhinal cortices, and the presubiculum; Goldman-Rakic et al., 1984; Selemon and Goldman-Rakic, 1988).

### Functional implications

The recent demonstration of "head-direction cells" in the presubiculum of rodents (Muller et al., 1996; Taube et al., 1996) and primates (Rolls, 1989; Robertson et al., 1999) suggests that the presubiculum may be closely involved in spatial and memory functions, such as navigation and path integration. These functions could critically depend on the connections from the IPL, whose role in

visuospatial processes is well known (Burgess et al., 1997). Further experiments will be necessary, however, to determine the structural and functional interactions of these connections with the dense inputs received by the presubiculum from other regions, including prefrontal (Goldman-Rakic et al., 1984; Selemon and Goldman-Rakic, 1988), cingulate (Pandya et al., 1981), and superior temporal (Amaral et al., 1983) cortices and subcortical centers, such as the anterior thalamus, basal amygdaloid nucleus, claustrum, and medial pulvinar (Shipley and Sorensen, 1975; Niimi, 1978; Krayniak et al., 1979; Aggleton, 1986; Amaral and Insausti, 1990).

The hippocampal formation and neocortical areas, as remarked in other studies (Goldman-Rakic et al., 1984), are interlinked by multiple channels. Our results emphasize that the posterior IPL has at least three moderately direct levels of access to the hippocampal formation (Fig. 20). Most direct are 1) the projections terminating in CA1 (Rockland and Van Hoesen, 1999; this report) and 2) those terminating in the perirhinal cortex and adjoining EC. In addition, there are 3) abundant indirect pathways to the EC from parietal-recipient regions in area TF and the presubiculum (Van Hoesen and Pandya, 1975; Van Hoesen, 1982; Seltzer and Pandya, 1984; Suzuki and Amaral, 1994a) as well as in the superior temporal sulcus (Insausti et al., 1987; Good and Morrison, 1995) and the prefrontal cortex (Selemon and Goldman-Rakic, 1988). Many of these projections terminate contralaterally and ipsilaterally. The medial pulvinar, which receives projections from the IPL and projects to both the presubiculum and the EC, constitutes another major subcortical circuit.

There are at least two interpretations of this redundant multiplicity of interconnections. One possibility is that each projection may be specialized to convey highly specific information to the hippocampus. This was suggested by Goldman-Rakic et al. (1984) in their demonstration that prefrontal projections had two pathways, through the presubiculum and the parahippocampal cortex, into the hippocampal formation. Earlier studies of parietal-to-hippocampal connections similarly emphasized dual pathways through the presubiculum and the parahippocampal cortex (Seltzer and Van Hoesen, 1979; Seltzer and Pandya, 1984). Although it may still be convenient to consider the presubiculum and area TF as somehow "in parallel," another, more likely possibility is that there is a more interactive, integrated architecture. The discovery that single IPL axons can branch to area TF, the perirhinal-entorhinal cortices, and the presubiculum would support this conclusion, as does the sheer density of the multiple pathways, which are well beyond two.

### Convergence of parietal and temporal connections

In the context of visual perception, the relative separation of parietal and temporal processing streams ("dorsal" and "ventral" streams) has been a useful concept (Morel and Bullier, 1990). In contrast, the parietal and temporal subsystems dedicated to visuospatial and memory processing appear to share several points of convergence. Area 7a and area TF, in addition to their own reciprocal interconnections (Cavada and Goldman-Rakic, 1989; Andersen et al., 1990; Martin-Elkins and Horel, 1992), send partially convergent connections to CA1 (Rockland and Van Hoesen, 1999) and to the adjoining parts of the perirhinal and entorhinal cortices. Ventromedial area TE,

which may be part of memory-related systems (Martin-Elkins and Horel, 1992), also projects to CA1 (Yukie and Iwai, 1988; Rockland and Van Hoesen, 1999; however, see also Suzuki and Amaral, 1990), to the border between the perirhinal and entorhinal cortices, and (seemingly unlike area TF) to the presubiculum as well. The convergence of projections from area 7a and ventromedial temporal areas at the border of perirhinal and entorhinal cortices may be significant for the marked impairment in visual recognition that results from ablations of the perirhinal region (Meunier et al., 1993; Suzuki et al., 1993; Buckley and Gaftan, 1998). It is worth noting, however, that rhinal lesions would also interrupt connections from the presubiculum to the rhinal cortex.

### CONCLUSIONS

The entorhinal and perirhinal cortices have long been accorded privileged status in the communication between neocortical areas and the hippocampal formation, with particular emphasis on temporal cortical and parahippocampal pathways. Although, in fact, there is massive convergence of temporal cortical systems in the peri- and entorhinal cortices, what has become the standard view overlooks the fact that the presubiculum is also a component of the parahippocampal gyrus and itself is a major source of input to the EC. Presubicular input is dominated by the frontal and parietal lobes and the parts of the cingulate gyrus that are interconnected with them. Factoring in this presubicular input, the EC emerges all the more as a cortical area influenced by all lobes. Finally, the divergence of axon collaterals from the IPL adds a new level of integration to the corticohippocampal architecture and calls for careful reanalysis of the ventromedial temporal networks.

### ACKNOWLEDGMENTS

The authors thank Tina Knutson for histological support, Diane Topinka for article preparation, and Pope Yamada for assistance with photography and graphics.

### LITERATURE CITED

Aggleton JP. 1986. A description of the amygdalo-hippocampal interconnections in the macaque monkey. *Exp Brain Res* 64:515-526.

Amaral DG, Insausti R. 1990. Hippocampal formation. In: Paxinos G, editor. *The human nervous system*. New York: Academic Press. p 711-801.

Amaral DG, Insausti R, Cowan WM. 1983. Evidence for a direct projection from the superior temporal gyrus to the entorhinal cortex in the monkey. *Brain Res* 275:263-277.

Amaral DG, Insausti R, Cowan WM. 1984. The commissural connections of the monkey hippocampal formation. *J Comp Neurol* 224:307-336.

Amaral DG, Insausti R, Cowan WM. 1987. The entorhinal cortex of the monkey: I. Cyto-architectonic organization. *J Comp Neurol* 264:326-355.

Andersen RA, Asanuma C, Essick G, Siegel RM. 1990. Corticocortical connections of anatomically and physiologically defined subdivisions within the inferior parietal lobule. *J Comp Neurol* 296:65-113.

Bakst I., Morrison JH, Amaral DG. 1985. The distribution of somatostatin-like immunoreactivity in the monkey hippocampal formation. *J Comp Neurol* 236:423-442.

Barbas H. 1995. Pattern in the cortical distribution of prefrontally directed neurons with divergent axons in the rhesus monkey. *Cereb Cortex* 2:158-165.

Blasdel GG, Lund JS. 1983. Termination of afferent axons in macaque striate cortex. *J Neurosci* 3:1389-1413.

- Brandt HM, Apkarian AV. 1992. Biotin-dextran: a sensitive anterograde tracer for neuroanatomic studies in rat and monkey. *J Neurosci Methods* 45:35–40.
- Buckley MJ, Gaffan D. 1998. Perirhinal cortex ablation impairs visual object identification. *J Neurosci* 18:2268–2275.
- Bullier J, Kennedy H. 1987. Axonal bifurcation in the visual system. *Trends Neurosci* 10:205–210.
- Burgess N, Jeffery KJ, O'Keefe J. 1997. What are the parietal and hippocampal contributions to spatial cognition. *Phil Trans R Soc London B* 352:1395–1543.
- Cavada C, Goldman-Rakic PS. 1989. Posterior parietal cortex in rhesus monkey: I. Parcellation of areas based on distinctive limbic and sensory corticocortical connections. *J Comp Neurol* 287:393–421.
- Ding SL, Van Hoesen GW, Rockland KS. 1999. Parietal connections to the presubiculum terminate with large arbors and branch widely to other areas. *Soc Neurosci Abstr* 25:1901.
- Felleman DJ, Xiao Y, McClelland E. 1997. Modular organization of occipito-temporal pathways: cortical connections between visual area 4 and visual area 2 and posterior inferotemporal ventral area in macaque monkeys. *J Neurosci* 17:3185–3200.
- Freund TF, Martin KAC, Soltesz I, Somogyi P, Whitteridge D. 1989. Arborization pattern and postsynaptic targets of physiologically identified thalamocortical afferents in striate cortex of the macaque monkey. *J Comp Neurol* 289:315–336.
- Gloor P. 1997. The temporal lobe and limbic system. New York: Oxford University Press.
- Goldman-Rakic PS, Selemon LD, Schwartz ML. 1984. Dual pathways connecting the dorsolateral prefrontal cortex with the hippocampal formation and parahippocampal cortex in the rhesus monkey. *Neuroscience* 12:719–743.
- Good PF, Morrison JH. 1995. Morphology and kainate-receptor immunoreactivity of identified neurons within the entorhinal cortex projecting to superior temporal sulcus in the cynomolgus monkey. *J Comp Neurol* 357:25–35.
- Insausti R, Amaral DG, Cowan WM. 1987. The entorhinal cortex of the monkey. II. Cortical afferents. *J Comp Neurol* 264:356–395.
- Kennedy H, Bullier J. 1985. A double-labelling investigation of the afferent connectivity to cortical areas V1 and V2 of the macaque monkey. *J Neurosci* 5:2815–2830.
- Kosel KC, Van Hoesen GW, Rosene DL. 1982. Non-hippocampal cortical projections from the entorhinal cortex in the rat and rhesus monkey. *Brain Res* 244:201–213.
- Krayniak PF, Siegel A, Meibach RC, Fruchtmann D, Scrimenti M. 1979. Origin of the fornix system in the squirrel monkey. *Brain Res* 160:401–411.
- Lorente de No R. 1934. Studies on the structure of the cerebral cortex. II. Continuation study of the ammonic system. *J Psychol Neurol* 46:113–177.
- Martin-Elkins CL, Horel JA. 1992. Cortical afferents to behaviorally defined regions of the inferior temporal and parahippocampal gyri as demonstrated by WGA-HRP. *J Comp Neurol* 321:177–192.
- Meunier M, Bachevalier J, Mishkin M, Murray EA. 1993. Effects on visual recognition of combined and separate ablations of the entorhinal and perirhinal cortex in rhesus monkeys. *J Neurosci* 13:5418–5432.
- Morel A, Bullier J. 1990. Anatomical segregation of two cortical visual pathways in the macaque monkey. *Vis Neurosci* 4:555–578.
- Morris R, Pandya DN, Petrides M. 1999. Fiber system linking the mid-dorsolateral frontal cortex with the retrosplenial/presubicular region in the rhesus monkey. *J Comp Neurol* 407:183–192.
- Muller RU, Ranck JB, Taube JS. 1996. Head direction cells: properties and functional significance. *Curr Opin Neurobiol* 6:196–206.
- Nakamura H, Gattass R, Desimone R, Ungerleider LG. 1993. The modular organization of projections from areas V1 and V2 to areas V4 and TEO in macaques. *J Neurosci* 13:3681–3691.
- Niimi M. 1978. Cortical projections of the anterior thalamic nuclei in the cat. *Exp Brain Res* 31:403–416.
- Pandya DN, Seltzer B. 1982. Intrinsic connections and architectonic of posterior parietal cortex in the rhesus monkey. *J Comp Neurol* 204:196–210.
- Pandya DN, Van Hoesen GW, Mesulam M-M. 1981. Efferent connections of the cingulate gyrus in the rhesus monkey. *Exp Brain Res* 42:319–330.
- Robertson RG, Rolls ET, Georges-François P, Panzeri S. 1999. Head direction cells in the primate pre-subiculum. *Hippocampus* 9:206–219.
- Rockland KS. 1997. Elements of cortical architecture: hierarchy revisited. In: Rockland KS, Kaas JH, Peters A, editors. *Cerebral cortex*, volume 12. Extrastriate cortex in primates. New York: Plenum Press. p 243–287.
- Rockland KS, Drash GW. 1996. Collateralized divergent feedback connections that target multiple cortical areas. *J Comp Neurol* 373:529–548.
- Rockland KS, Van Hoesen GW. 1994. Direct temporal-occipital feedback connections to striate cortex (V1) in the macaque monkey. *Cereb Cortex* 4:300–313.
- Rockland KS, Van Hoesen GW. 1999. Some temporal and parietal cortical connections converge in CA1 of the primate hippocampus. *Cereb Cortex* 9:232–237.
- Rockland KS, Saleem KS, Tanaka K. 1994. Divergent feedback connections from area V4 and TEO in the macaque. *Vis Neurosci* 11:579–600.
- Rolls ET. 1989. Hippocampal neurons in the monkey with activity related to the place in which a stimulus is shown. *Neuroscience* 9:1835–1845.
- Rosene DL, Van Hoesen GW. 1987. The hippocampal formation of the primate brain, a review of some comparative aspects of cytoarchitecture and connections. In: Jones EG, Peters A, editors. *Cerebral cortex*, volume 6. New York: Plenum Press. p 345–455.
- Saleem KS, Tanaka K. 1996. Divergent projections from the anterior inferotemporal area TE to the perirhinal and entorhinal cortices in the macaque monkey. *J Neurosci* 16:4757–4775.
- Selemon LD, Goldman-Rakic PS. 1988. Common cortical and subcortical targets of the dorsolateral prefrontal and posterior parietal cortices in the rhesus monkey: evidence for a distributed neural network subserving spatially guided behavior. *J Neurosci* 8:4049–4068.
- Seltzer B, Pandya DN. 1984. Further observations on parieto-temporal connections in the rhesus monkey. *Exp Brain Res* 55:301–312.
- Seltzer B, Van Hoesen GW. 1979. A direct inferior parietal lobule projection to the presubiculum in the rhesus monkey. *Brain Res* 179:157–161.
- Shiple MT, Sorensen KE. 1975. On the laminar organization of the anterior thalamus projections to the presubiculum in the guinea pig. *Brain Res* 86:473–477.
- Sik A, Tamamaki N, Freund TF. 1993. Complete axon arborization of a single CA3 pyramidal cell in the rat hippocampus, and its relationship with postsynaptic parvalbumin-containing interneurons. *Eur J Neurosci* 5:1719–1728.
- Suzuki WA, Amaral DG. 1990. Cortical inputs to the CA1 field of the monkey hippocampus originate from the perirhinal and parahippocampal cortex but not from area TE. *Neurosci Lett* 115:43–48.
- Suzuki WA, Amaral DG. 1994a. Perirhinal and parahippocampal cortices of the macaque monkey: cortical afferents. *J Comp Neurol* 350:497–533.
- Suzuki WA, Amaral DG. 1994b. Topographic organization of the reciprocal connections between the monkey entorhinal cortex and the perirhinal and parahippocampal cortices. *J Neurosci* 14:1856–1877.
- Suzuki WA, Zola-Morgan S, Squire LR, Amaral DG. 1993. Lesions of the perirhinal and parahippocampal cortices in the monkey produce long-lasting memory impairment in the visual and tactile modalities. *J Neurosci* 13:2430–2451.
- Tamamaki N, Nojyo Y. 1993. Projection of the entorhinal layer II neurons in the rat as revealed by intracellular pressure-injection of neurobiotin. *Hippocampus* 3:471–480.
- Taube JS, Goodridge JP, Golob EJ, Dudchenko PA, Stackman RW. 1996. Processing the head direction signal: a review and commentary. *Brain Res Bull* 40:477–486.
- Van Hoesen GW. 1982. The parahippocampal gyrus. New observations regarding its cortical connections in the monkey. *Trends Neurosci* 5:345–350.
- Van Hoesen GW, Pandya DN. 1975. Some connections of the entorhinal (area 28) and perirhinal (area 35) cortices of the rhesus monkey. I. Temporal lobe afferents. *Brain Res* 95:1–24.
- Van Hoesen GW, Pandya DN, Butters N. 1972. Cortical afferents to the entorhinal cortex of the rhesus monkey. *Science* 175:1471–1473.
- Veenman CL, Reiner A, Honig MG. 1992. Biotinylated dextran amine as an anterograde tracer for single and double-labeling studies. *J Neurosci Methods* 41:239–254.
- Von Bonin G, Bailey P. 1947. The neocortex of *Macaca mulatta*. Urbana, IL: The University of Illinois Press.
- Webster MJ, Bachevalier J, Ungerleider LG. 1994. Connections of inferior temporal areas TEO and TE with parietal and frontal cortex in macaque monkeys. *Cereb Cortex* 4:470–483.
- Wellman BJ, Rockland KS. 1997. Divergent cortical connections to entorhinal cortex from area TF in the macaque. *J Comp Neurol* 389:361–376.
- Yukie M, Iwai E. 1988. Direct projections from the ventral TE area of the inferotemporal cortex to hippocampal field CA1 in the monkey. *Neurosci Lett* 88:6–10.